ELECTROCHIMICA Acta

THE JOURNAL OF THE INTERNATIONAL SOCIETY
OF ELECTROCHEMISTRY

AUTHOR INDEX
SUBJECT INDEX

VOLUME 45 (2000)

PERGAMON

PERGAMON

Electrochimica Acta 45 (2000) 1–28

ELECTROCHIMICA Acta

www.elsevier.nl/locate/electacta

Author Index for Volume 45 (2000)

A

Aabloo, A., Klintenberg, M. and Thomas, J.O.
Molecular dynamics simulation of a polymer–inorganic interface, 1425
Aaron, J.-J., see Sakmeche, N., 1921
Abdelmula, E., see Beck, F., 3423
Abe, M.
Ferrite plating: a chemical method preparing oxide magnetic films at 24–100°C, and its applications, 3337
Abe, T., Goto, T., Ohzeki, K. and Kaneko, M.
Electrocatalysis for proton reduction by a coated Nafion® membrane dispersing ruthenium moieties, 4009
Abe, T., see Funabiki, A., 865
Abe, T., see Inaba, M., 99
Abe, T., see Zhang, J., 399
Abraham, K.M., see Gu, G.Y., 3127
Abrantes, L.M. and Correia, J.P.
Polypyrrole incorporating electroless nickel, 4179
Abrantes, L.M., González, J., Molina, A. and Saavedra, F.
Application of cyclic reciprocal derivative chronopotentiometry with programmed currents to the study of the reversibility of electrode processes, 457
Abrantes, L.M., see Molina, A., 761
Acosta, J.L., see Morales, E., 1049
Adžić, R.R. and Wang, J.X.
Structure and inhibition effects of anion adlayers during the course of O_2 reduction, 4203
Aeiyach, S., see Sakmeche, N., 1921
Agostiano, A., Caselli, M., Cosma, P. and Della Monica, M.
Electrochemical investigation of the interaction of different mediators with the photosynthetic reaction center from *Rhobobacter sphaeroides*, 1821
Ahlers, C.B. and Talbot, J.B.
Voltammetric behavior of zeolite-modified electrodes fabricated by electrophoretic deposition, 3379
Ahn, W.Y. and Bae, Y.C.
Phase behaviors of solid polymer electrolyte–salt systems: the effect of pressure, 3157
Aihara, M., see Hassel, A.W., 4673
Aihara, Y., Arai, S. and Hayamizu, K.
Ionic conductivity, DSC and self diffusion coefficients of lithium, anion, polymer, and solvent of polymer gel electrolytes: the structure of the gels and the diffusion mechanism of the ions, 1321
Aihara, Y., see Hayamizu, K., 1313
Aikawa, H., see Furuya, N., 4251
Alcaraz, M.-L., see Martínez-Ortiz, F., 387
Aldinger, F., see Näfe, H., 1631
Alloin, F., Bayoud, S., Azimipour, B., Reibel, L. and Sanchez, J.-Y.
Electrochemical investigation of lithium aromatic sulfonyl imide salts, 1193
Alloin, F., see Saunier, J., 1255
Allongue, P., Henry de Villeneuve, C. and Pinson, J.
Structural characterization of organic monolayers on Si⟨111⟩ from capacitance measurements, 3241
Allongue, P., Henry de Villeneuve, C., Morin, S., Boukherroub, R. and Wayner, D.D.M.
The preparation of flat H–Si(111) surfaces in 40% NH_4F revisited, 4591
Alonso-Vante, N., Borthen, P., Fieber-Erdmann, M., Strehblow, H.-H. and Holub-Krappe, E.
An in situ grazing incidence X-ray absorption study of ultra thin Ru_xSe_y cluster-like electrocatalyst layers, 4227
Amadelli, R., Armelao, L., Velichenko, A.B., Nikolenko, N.V., Girenko, D.V., Kovalyov, S.V. and Danilov, F.I.
Oxygen and ozone evolution at fluoride modified lead dioxide electrodes, 713
Amadelli, R., see Velichenko, A.B., 4341
Amatucci, G., Du Pasquier, A., Blyr, A., Zheng, T. and Tarascon, J.-M.
The elevated temperature performance of the $LiMn_2O_4$/C system: failure and solutions, 255
Andolfatto, F., see Pauporté, T., 431
Andreev, Y.G. and Bruce, P.G.
Polymer electrolyte structure and its implications, 1417

PII: S0013-4686(01)00500-X

Andreu, R., see Calvente, J.J., 3087
Angell, C.A., see Zhang, S., 1229
Angert, N., see Dobrev, D., 3117
Antoine, O., Bultel, Y., Ozil, P. and Durand, R.
Catalyst gradient for cathode active layer of proton exchange membrane fuel cell, 4493
Antonucci, V., see Aricò, A.S., 4319
Aoki, K. and Tokida, A.
Resistance of solution without supporting electrolyte under the reduction of HCl, 3483
Aoki, T., see Ohzuku, T., 151
Aono, Y., see Taniguchi, I., 2843
Appetecchi, G.B. and Passerini, S.
PEO-carbon composite lithium polymer electrolyte, 2139
Appetecchi, G.B., Croce, F., Marassi, R., Persi, L., Romagnoli, P. and Scrosati, B., 23
Appetecchi, G.B., Croce, F., Persi, L., Ronci, F. and Scrosati, B.
Transport and interfacial properties of composite polymer electrolytes, 1481
Arai, H., see Okada, S., 329
Arai, K., Sato, T., Tamanouchi, H., Ohtomo, M., Takamura, K., Sueoka, T. and Kusu, F.
Electrolysis of 2-methyl-1,4-naphthoquinone and 3,5-di-*tert*-butyl-1,2-benzoquinone using the flow-cell system with a column electrode, 3029
Arai, K., see Fuse, T., 2933
Arai, S., see Aihara, Y., 1321
Arai, S., see Hayamizu, K., 1313
Arakelyan, V.M., see Aroutiounian, V.M., 1999
Araki, F., see Morita, M., 1335
Arbizzani, C., Mastragostino, M. and Soavi, F.
Polythiophene S,S dioxides: an investigation on electrochemical doping, 2273
Argyropoulos, P., Scott, K. and Taama, W.M.
The effect of operating conditions on the dynamic response of the direct methanol fuel cell, 1983
Argyropoulos, P., see Scott, K., 945
Aricò, A.S., Creti, P., Modica, E., Monforte, G., Baglio, V. and Antonucci, V.
Investigation of direct methanol fuel cells based on unsupported Pt–Ru anode catalysts with different chemical properties, 4319
Armelao, L., see Amadelli, R., 713
Armstrong, A.R., Robertson, A.D. and Bruce, P.G., 285
Armstrong, F.A. and Wilson, G.S.
Recent developments in faradaic bioelectrochemistry, 2623
Armyanov, S.
Crystallographic structure and magnetic properties of electrodeposited cobalt and cobalt alloys, 3323
Arof, A.K., see Jacob, M.M.E., 1701
Aroutiounian, V.M., Arakelyan, V.M., Shahnazaryan, G.E., Stepanyan, G.M., Turner, J.A. and Kocha, S.S.
Investigations of the $Fe_{1.99}Ti_{0.01}O_3$–electrolyte interface, 1999
Asaka, K. and Oguro, K.
Bending of polyelectrolyte membrane–platinum composite by electric stimuli III: self-oscillation, 4517
Asakura, K., see Okada, S., 329
Ascone, I., see Giorgetti, M., 4475
Aucouturier, M., see Zwilling, V., 921
Aurbach, D., Markovsky, B., Weissman, I., Levi, E. and Ein-Eli, Y., 67
Aurbach, D., see Levi, M.D., 1781
Aurbach, D., see Levi, M.D., 167
Aurbach, D., Weissman, I., Zaban, A. and Dan, P.
On the role of water contamination in rechargeable Li batteries, 1135
Aurousseau, M., see Chatenet, M., 2823
Avaca, L.A., see de Oliveira-Sousa, A., 4467
Averina, Y., see Guterman, V., 873
Awata, H., see Iwahori, T., 1509
Azimipour, B., see Alloin, F., 1193

B

Bach, S., Belair, S., Cachet-Vivier, C., Pereira-Ramos, J.P., Sanchez, L., Lavela, P. and Tirado, J.L.
Electrochemical proton insertion in $Mn_{2.2}Co_{0.27}O_4$ from aqueous borate solution, 931
Badiali, J.P., see Stafiej, J., 3489
Bae, Y.C., see Ahn, W.Y., 3157
Baglio, V., see Aricò, A.S., 4319
Bahn, C.S., see McGraw, J.M., 187
Baier, S., see Giesen, M., 527
Baker, R.T., see Gharbage, B., 2095
Bandaranayake, P.W.S.K., see Perera, K., 1361
Baños, L., see González, M., 741
Barbero, C., Calvo, E.J., Etchenique, R., Morales, G.M. and Otero, M.
An EQCM electroacoustic study of poly(vinylferrocene) modified electrodes in different aqueous electrolytes, 3895
Barbier, J., see Lamy-Pitara, E., 4299
Barbier, J., see Quiroz, M.A., 4291
Barker, J.
In-situ measurement of the thickness changes associated with cycling of prismatic lithium ion batteries based on $LiMn_2O_4$ and $LiCoO_2$, 235
Barrado, E., Prieto, F., Castrillejo, Y. and Medina, J.
Chemical and electrochemical characterization of lead ferrites produced in the purification of lead-bearing wastewater, 1105
Barth, M., Guilerez, S., Bidan, G., Bras, G. and Łapkowski, M.

Electrochemical investigation of regioregular alkyl substituted oligothiophenes, 4409
Bartlett, P.N., see Gollas, B., 3711
Baturina, O.A., see Sottomayor, M.J., 775
Bayoud, S., see Alloin, F., 1193
Beck, F., Abdelmula, E. and Dahlhaus, M.
Anodic deposition of composites with a matrix of intrinsically conducting polymers, 3423
Beck, F. and Rüetschi, P.
Rechargeable batteries with aqueous electrolytes, 2467
Beck, F., Kaiser, W. and Krohn, H.
Boron doped diamond (BDD)-layers on titanium substrates as electrodes in applied electrochemistry, 4691
Beck, F., see Chromik, R., 2175
Becker, J.Y., see Rogers, K.R., 4373
Beerbom, M., Henrion, O., Klein, A., Mayer, T. and Jaegermann, W.
XPS analysis of wet chemical etching of GaAs(110) by Br_2–H_2O: comparison of emersion and model experiments, 4663
Belaïdi, A., see Chazalviel, J.-N., 3205
Belair, S., see Bach, S., 931
Bélanger, D., see Fusalba, F., 3877
Belca, I., Kasalica, B., Zekovic, L., Jovanic, B. and Vasilic, R.
The galvanoluminescence spectra of porous oxide layers formed by aluminum anodization in oxalic acid, 993
Belca, I.D., Zekovic, L.D., Jovanic, B., Ristovski, G. and Ristovski, L.
The theory of galvanoluminescence in the anodic oxide films obtained by aluminum anodization in ammonium tartrate, 4059
Benedetti, A.V., Cabot, P.L., Garrido, J.A. and Moreira, A.H.
Effect of welding on the microstructure and electrochemical corrosion of Al–Zn–Mg–Fe alloys, 2187
Benito, D., see Sanmatías, A., 797
Berlouis, L.E.A., Wark, A.W., Cuickshank, F.R., Pugh, D. and Brevet, P.F.
Interference between second harmonic waves in an anodically grown cadmium sulphide thin film, 623
Berlouis, L.E.A., see Quijada, C., 1847
Berrettoni, M., see Giorgetti, M., 4475
Besenhard, J.O., see Winter, M., 31
Bessone, J.B., see Saidman, S.B., 3151
Bezdička, P., Grygar, T., Klápště, B. and Vondrák, J.
MnO_x/C composites as electrode materials. I. Synthesis, XRD and cyclic voltammetric investigation, 913
Biallozor, S., see Zalewska, T., 4031
Bidan, G., see Barth, M., 4409
Biensan, P., see Broussely, M., 3
Biensan, P., see Guerin, K., 1607
Billaud, D., see Naji, A., 1893
Billaud, D., see Thomas, P., 423
Billaud, D., Thevenot, L. and Willmann, P.
New electrochemical and chemical routes for the synthesis of lithium rich graphite intercalation compounds, 59
Biran, C., see Jouikov, V., 1015
Birss, V.I., see Xia, S.J., 3659
Bishop, A.G., see Every, H., 1279
Bjerrum, N.J., see Qingfeng, L., 4219
Blyr, A., see Amatucci, G., 255
Böhm, S., McMurray, H.N., Powell, S.M. and Worsley, D.A.
Photoelectrochemical investigation of corrosion using scanning electrochemical techniques, 2165
Bojinov, M., Fabricius, G., Kinnunen, P., Laitinen, T., Mäkelä, K., Saario, T. and Sundholm, G.
The mechanism of transpassive dissolution of Ni–Cr alloys in sulphate solutions, 2791
Bojinov, M., Fabricius, G., Laitinen, T., Mäkelä, K., Saario, T. and Sundholm, G.
Coupling between ionic defect structure and electronic conduction in passive films on iron, chromium and iron–chromium alloys, 2029
Bollo, S., see Núñez-Vergara, L.J., 3555
Boodts, J.F.C., see Da Silva, L.M., 2719
Bordeau, M., see Jouikov, V., 1015
Borgwarth, K., see Hess, C., 3725
Börjesson, L., see Carlsson, P., 1449
Borkowska, Z., see Stafiej, J., 3489
Borkowska, Z., see Tymosiak-Zielińlska, A., 3105
Borrás, C.A., Romagnoli, R. and Lezna, R.O.
In-situ spectroelectrochemistry (UV–visible and infrared) of anodic films on iron in neutral phosphate solutions, 1717
Borthen, P., see Alonso-Vante, N., 4227
Botte, G.G., Subramanian, V.R. and White, R.E.
Mathematical modeling of secondary lithium batteries, 2595
Boukherroub, R., see Allongue, P., 4591
Bouvier, S., see Gu, G.Y., 3127
Bouwkamp-Wijnoltz, A.L., Visscher, W., van Veen, J.A.R. and Tang, S.C.
Electrochemical reduction of oxygen: an alternative method to prepare active CoN_4 catalysts, 379
Bozzini, B., Brevaglieri, B., Cavallotti, P.L., Giovannelli, G. and Natali, S.
Hydrodynamic problems related to the electrodeposition of AuCu/B_4C composites, 3431
Brabec, V.
DNA sensor for the determination of antitumor platinum compounds, 2929
Bradley, P.E. and Landolt, D.
Pulse-plating of copper–cobalt alloys, 1077
Bras, G., see Barth, M., 4409
Breslin, C.B., see Rudd, A.L., 1571

Breslin, C.B., see Rudd, A.L., 4015
Brett, D.J.L., see Wilde, C.P., 3649
Brevaglieri, B., see Bozzini, B., 3431
Brevet, P.F., see Berlouis, L.E.A., 623
Brillas, E., Carrasco, J., Oliver, R., Estrany, F., Vilar, J. and Morlans, J.M.
Electropolymerization of 2,5-di-(-2-thienyl)-pyrrole in ethanolic medium. Effect of solution stirring on doping with perchlorate and chloride ions, 4049
Brodin, A., see Ericson, H., 1409
Bron, M. and Holze, R.
The adsorption of thiocyanate ions at gold electrodes from an alkaline electrolyte solution: a combined in situ infrared and Raman spectroscopic study, 1121
Brouant, P., see Dicu, D., 3951
Broussely, M., Biensan, P. and Simon, B.
Lithium insertion into host materials: the key to success for Li ion batteries, 3
Bruce, P.G., see Andreev, Y.G., 1417
Bruce, P.G., see Armstrong, A.R., 285
Bruckenstein, S., Brzezinska, K. and Hillman, A.R.
EQCM studies of polypyrrole films. 1. Exposure to aqueous sodium tosylate solutions under thermodynamically permselective conditions, 3801
Brzezinska, K., see Bruckenstein, S., 3801
Budevski, E., Staikov, G. and Lorenz, W.J.
Electrocrystallization: Nucleation and growth phenomena, 2559
Buess-Herman, C., see Van krieken, M., 675
Buffle, J., see Pei, J., 1581
Buiel, E. and Dahn, J.R.
Li-insertion in hard carbon anode materials for Li-ion batteries, 121
Bukowska, J., see Janik-Czachor, M., 3295
Bultel, Y., see Antoine, O., 4493
Bund, A. and Schwitzgebel, G.
Investigations on metal depositions and dissolutions with an improved EQCMB based on quartz crystal impedance measurements, 3703
Bunk, O., see Ziegler, J.C., 4599
Burgess, J.D., see Rhoten, M.C., 2855
Burkal'tseva, L.A., see Pshenichnikov, A.G., 4143
Burke, L.D., Collins, J.A., Horgan, M.A., Hurley, L.M. and O'Mullane, A.P.
The importance of the active states of surface atoms with regard to the electrocatalytic behaviour of metal electrodes in aqueous media, 4127
Buttry, D.A., see Shouji, E., 3757
Bzducha, W., see Florjańczyk, Z., 1203
Bzducha, W., see Florjańczyk, Z., 3563

C

Cabot, P.L., see Benedetti, A.V., 2187
Cachet-Vivier, C., see Bach, S., 931
Cahan, B.D., see Totir, D.A., 161
Calvente, J.J., Gil, M.L., Sánchez, M.D., Andreu, R. and de Pablos, F.
Voltammetry of surface redox processes perturbed by a father–son reaction, 3087
Calvo, E.J., see Barbero, C., 3895
Canalas, M.T., see Collins, C.M., 2049
Cao, C.N., see Yan, C.W., 2815
Capiglia, C., Saito, Y., Yamamoto, H., Kageyama, H. and Mustarelli, P.
Transport properties and microstructure of gel polymer electrolytes, 1341
Carlen, M., see Kötz, R., 2483
Carlos, L.D., Sa Ferreira, R.A. and de Zea Bermudez, V.
An intra-Nd^{3+} visible to infrared conversion process in hybrid xerogels, 1555
Carlos, L.D., see Silva, M.M., 1467
Carlsson, P., Swenson, J., Börjesson, L., McGreevy, R.L., Jacobsson, P., Torell, L.M. and Howells, W.S.
Neutron diffraction investigations of the cation coordination in an amorphous polymer electrolyte, PPO–$LiClO_4$, 1449
Carrasco, J., see Brillas, E., 4049
Carré, B., see Geoffroy, I., 2019
Carrero, H., Gao, J., Rusling, J.F., Lee, C.-W. and Fry, A.J.
Direct and catalyzed electrochemical syntheses in microemulsions, 503
Carrillo Ramiro, I., see González-Tejera, M.J., 1973
Casella, I.G. and Guascito, M.R.
Electrochemical preparation of a composite gold–cobalt electrode and its electrocatalytic activity in alkaline medium, 1113
Caselli, M., see Agostiano, A., 1821
Cass, A.E.G., see Glidle, A., 3823
Castrillejo, Y., see Barrado, E., 1105
Cattarin, S., Frateur, I., Guerriero, P. and Musiani, M.
Electrodeposition of $PbO_2 + CoO_x$ composites by simultaneous oxidation of Pb^{2+} and Co^{2+} and their use as anodes for O_2 evolution, 2279
Cattarin, S., see Decker, F., 4607
Cavallotti, P.L., see Bozzini, B., 3431
Ceder, G. and Van der Ven, A.
Phase diagrams of lithium metal oxides: investigations from first principles, 131
Cembrano, J., see Rogers, K.R., 4373
Cesiulis, H., see Donten, M., 3389
Chambers, J.Q., see Kertesz, V., 1095
Chang, K.-H., see Hu, C.-C., 2685
Chang, M.-R., see Zen, J.-M., 1691
Chang, Z., see Zhang, S., 1229
Chartier, P., see Ríos, E., 4431
Chartier, P., see Singh, R.N., 1911

Chatenet, M., Aurousseau, M. and Durand, R.
Electrochemical measurement of the oxygen diffusivity and solubility in concentrated alkaline media on rotating ring-disk and disk electrodes—application to industrial chlorine-soda electrolyte, 2823
Chazalviel, J.-N., Belaïdi, A., Safi, M., Maroun, F., Erné, B.H. and Ozanam, F.
In situ semiconductor surface characterisation: a comparative infrared study of Si, Ge and GaAs, 3205
Che, Y., see Fei Wu, J., 987
Chen, A., see Hoon-Khosla, M., 611
Chen, P.-Y. and Sun, I.-W.
Electrochemical study of copper in a basic 1-ethyl-3-methylimidazolium tetrafluoroborate room temperature molten salt, 441
Chen, P.-Y. and Sun, I.-W.
Electrochemistry of Cd(II) in the basic 1-ethyl-3-methylimidazolium chloride/tetrafluoroborate room temperature molten salt, 3163
Chen, S. and Schell, M.
Excitability and multistability in the electrochemical oxidation of primary alcohols, 3069
Chen, S.-M. and Chiu, S.-W.
The electrocatalytic transformation of HS^-, $S_2O_3^{2-}$, $S_4O_6^{2-}$ and SO_3^{2-} to SO_4^{2-} by water-soluble iron porphyrins, 4399
Cheng, Y.F., Luo, J.L. and Wilmott, M.
Spectral analysis of electrochemical noise with different transient shapes, 1763
Cherginets, V.L. and Rebrova, T.P.
Studies of some acid–base equilibria in the molten eutectic mixture KCl–LiCl at 700°C, 469
Chialvo, A.C., see Marozzi, C.A., 2111
Chiu, S.-W., see Chen, S.-M., 4399
Cho, E.-A., Kim, C.-K., Kim, J.-S. and Kwon, H.-S.
Quantitative analysis of repassivation kinetics of ferritic stainless steels based on the high field ion conduction model, 1933
Cho, J., see Min, M.-k., 4211
Cho, K., see Min, M.-k., 4211
Chockalingam, S.C., see Kulandaisamy, S., 3047
Choi, B.K., Kim, Y.W. and Shin, H.K.
Ionic conduction in PEO–PAN blend polymer electrolytes, 1371
Choi, B.K., see Kim, Y.W., 1473
Chowdhury, P.B., see Kucernak, A.R., 4483
Christensen, P. and Hamnett, A.
In-situ techniques in electrochemistry — ellipsometry and FTIR, 2443
Christensen, P.A., see Reeve, R.W., 4237
Chromik, R. and Beck, F.
A quantitative discrimination between reversible Li^+-insertion and irreversible solvent oxidation at a lithium/manganese-spinel electrode, 2175
Chu, D., see Jiang, R., 4025
Chung, M.-H.
A numerical method for analysis of tertiary current distribution in unsteady natural convection multi-ion electrodeposition, 3959
Chung, T.D., see Kang, S.K., 2939
Cisneros-González, I., Oropeza-Guzmán, M.T. and González, I.
An electrochemical study of galena concentrate in perchlorate medium at pH 2.0: the influence of chloride ions, 2729
Claye, A. and Fischer, J.E.
Short-range order in disordered carbons: where does the Li go?, 107
Climent, V., Gómez, R. and Feliu, J.M.
Effect of increasing amount of steps on the potential of zero total charge of Pt(111) electrodes, 629
Clotet, A., see Curulla, D., 639
Coelho, V., see Sottomayor, M.J., 775
Colin, C., see Petit, M.A., 1953
Collins, C.M., Sotiriou-Leventis, C., Canalas, M.T. and Leventis, N.
A cyclic voltammetric study of the proton abstraction from selected aromatic ketones by superoxide, 2049
Collins, J.A., see Burke, L.D., 4127
Comiti, J., see Legrand, J., 1791
Comninellis, C., see Mousty, C., 451
Comtat, M., see Serpentini, C.-L., 1663
Contamin, O., Debiemme-Chouvy, C., Savy, M. and Scarbeck, G.
Oxygen electroreduction catalysis: effect of sulfur addition on cobalt tetraazaannulene precursors, 721
Conway, B.E. and Jerkiewicz, G.
Relation of energies and coverages of underpotential and overpotential deposited H at Pt and other metals to the 'volcano curve' for cathodic H_2 evolution kinetics, 4075
Cooper, J.M., see Glidle, A., 3823
Cordeiro, M.N.D.S., see Ignaczak, A., 659
Córdova, F., see Quiroz, M.A., 4291
Correia, A.N. and Machado, S.A.S.
Electrodeposition and characterisation of thin layers of Ni–Co alloys obtained from dilute chloride baths, 1733
Correia, J.P., see Abrantes, L.M., 4179
Cosma, P., see Agostiano, A., 1821
Courtney, I.A., Dunlap, R.A. and Dahn, J.R.
In-situ ^{119}Sn Mössbauer effect studies of the reaction of lithium with SnO and SnO:0.25 B_2O_3:0.25 P_2O_5 glass, 51
Crayston, J.A., see de Alwis, C., 2061
Cretì, P., see Aricò, A.S., 4319
Cristea, C., see Dicu, D., 3951
Croce, F., see Appetecchi, G.B., 23
Croce, F., see Appetecchi, G.B., 1481
Croguennec, L., see Delmas, C., 243

Cromie, T., see de Alwis, C., 2061
Cui, N. and Luo, J.L.
An AC impedance study of self-discharge mechanism of nickel–metal hydride (Ni–MH) battery using Mg_2Ni-type hydrogen storage alloy anode, 3973
Cuickshank, F.R., see Berlouis, L.E.A., 623
Curulla, D., Clotet, A., Ricart, J.M. and Illas, F.
Ab initio cluster model study of electric field effects for terminal and bridge bonded CO on Pt(100), 639

D

Dahlhaus, M., see Beck, F., 3423
Dahn, J.R., see Buiel, E., 121
Dahn, J.R., see Courtney, I.A., 51
Dai, J., Li, S.F.Y., Siow, K.S. and Gao, Z.
Synthesis and characterization of the hollandite-type MnO_2 as a cathode material in lithium batteries, 2211
Daikhin, L., Gileadi, E., Tsionsky, V., Urbakh, M. and Zilberman, G.
Slippage at adsorbate–electrolyte interface. Response of electrochemical quartz crystal microbalance to adsorption, 3615
Daikhin, L.I., Kornyshev, A.A. and Urbakh, M.
Effect of capillary waves on the double layer capacitance of the interface between two immiscible electrolytes, 685
Dakova, B., Martens, T. and Evers, M.
Electrochemical oxidation of [2H] benziso-1,2-thiazol-3-one mediated by chloride anions. Application to a new and expedient electrochemical synthesis of [2H] benziso-1,2-thiazol-3-one S-oxide, 4525
Damaskin, B.B., see Sottomayor, M.J., 775
Dan, P., see Aurbach, D., 1135
Danilov, F.I., see Amadelli, R., 713
Danilov, F.I., see Velichenko, A.B., 4341
Dao, L.H., see Song, H.-K., 2241
Darque-Ceretti, E., see Zwilling, V., 921
Da Silva, L.M., Boodts, J.F.C. and DeFaria, L.A.
'In situ' and 'ex situ' characterization of the surface properties of the RuO_2 $(x) + Co_3O_4$ $(1 - x)$ system, 2719
da Silva, M.A.S., see de Oliveira-Sousa, A., 4467
Datta, M. and Landolt, D.
Fundamental aspects and applications of electrochemical microfabrication, 2535
Dávila Jiménez, M.M., Elizalde, M.P., González, M. and Silva, R.
Electrochemical behaviour of nickel–polyester composite electrodes, 4187
Dávila, M.M., see González, M., 741
de Alwis, C., Crayston, J.A., Cromie, T., Eisenblätter, T., Hay, R.W., Lampeka, Y.D. and Tsymbal, L.V.
Cyclic voltammetry study of the electrocatalysis of carbon dioxide reduction by bis(polyazamacrocyclic) nickel complexes, 2061
Debiemme-Chouvy, C., see Contamin, O., 721
Decker, F., Pantano, E., Dini, D., Cattarin, S., Maffi, S. and Razzini, G.
Use of the bending-beam-method for the study of the anodic oxidation of Si in dilute fluoride media, 4607
De Cliff, S.V., see Wilde, C.P., 3649
DeFaria, L.A., see Da Silva, L.M., 2719
de Lima-Neto, P., see de Oliveira-Sousa, A., 4467
Della Monica, M., see Agostiano, A., 1821
Delmas, C., Ménétrier, M., Croguennec, L., Saadoune, I., Rougier, A., Pouillerie, C., Prado, G., Grüne, M. and Fournès, L.
An overview of the Li $(Ni,M)O_2$ systems: syntheses, structures and properties, 243
Del Pópolo, M.G., see Giménez, M.C., 699
de Montauzon, D., see Serpentini, C.-L., 1663
de Oliveira-Sousa, A., da Silva, M.A.S., Machado, S.A.S., Avaca, L.A. and de Lima-Neto, P.
Influence of the preparation method on the morphological and electrochemical properties of Ti/IrO_2-coated electrodes, 4467
de Pablos, F., see Calvente, J.J., 3087
Depre, L., Ingram, M., Poinsignon, C. and Popall, M.
Proton conducting sulfon/sulfonamide functionalized materials based on inorganic–organic matrices, 1377
Deslouis, C., Festy, D., Gil, O., Maillot, V., Touzain, S. and Tribollet, B.
Characterization of calcareous deposits in artificial sea water by impedances techniques: 2-deposit of $Mg(OH)_2$ without $CaCO_3$, 1837
Dessemond, L., see Vermoyal, J.J., 1039
de Tacconi, N.R., Rajeshwar, K. and Lezna, R.O.
Preparation, photoelectrochemical characterization, and photoelectrochromic behavior of metal hexacyanoferrate–titanium dioxide composite films, 3403
de Tacconi, N.R., see Myung, N., 3749
de Zea Bermudez, V., see Carlos, L.D., 1555
de Zea Bermudez, V., see Silva, M.M., 1467
Dhathathreyan, K.S., see Rajalakshmi, N., 4511
Diamantopoulou, A., see Sazou, D., 2753
Dickinson, A.J., see Reeve, R.W., 4237
Dicu, D., Muresan, L., Popescu, I.C., Cristea, C., Silberg, I.A. and Brouant, P.
Modified electrodes with new phenothiazine derivatives for electrocatyltic oxidation of NADH, 3951
Dini, D., see Decker, F., 4607
Di Noto, V., see Münchow, V., 1211
Dissanayake, M.A.K.L., see Perera, K., 1361
Dittrich, T., see Rappich, J., 4629
Doblhofer, K., see Eickes, C., 3623
Dobrev, D., Vetter, J., Angert, N. and Neumann, R.
Periodic reverse current electrodeposition of gold in an ultrasonic field using ion-track membranes as templates: growth of gold single-crystals, 3117

Dolata, M., see Janik-Czachor, M., 3295
Dong, S., see Liu, S., 1683
Donten, M., Cesiulis, H. and Stojek, Z.
Electrodeposition and properties of Ni–W, Fe–W and Fe–Ni–W amorphous alloys. A comparative study, 3389
Dražan, V., see Vetterl, V., 2961
Dretschkow, T. and Wandlowski, T.
An order–disorder–order adlayer transition of 2,2′-bipyridine on Au(111), 731
Duffy, N.W., Peter, L.M., Wang, R.L., Lane, D.W. and Rogers, K.D.
Electrodeposition and characterisation of CdTe films for solar cell applications, 3355
Dumestre, F., see Fabre, P.-L., 2697
Dumont, E., see Legrand, J., 1791
Dunlap, R.A., see Courtney, I.A., 51
Dunoguès, J., see Jouikov, V., 1015
Du Pasquier, A., see Amatucci, G., 255
Durand, R., see Antoine, O., 4493
Durand, R., see Chatenet, M., 2823
Durand, R., see Pauporté, T., 431
Dvořák, J., see Vetterl, V., 2961
Dygas, J.R., see Florjańczyk, Z., 3563

E

Edman, L., see Ferry, A., 1237
Ehret, A., Stuhl, L. and Spitler, M.T.
Variation of carboxylate-functionalized cyanine dyes to produce efficient spectral sensitization of nanocrystalline solar cells, 4553
Ehrlich, J., Ehrlich, T., Jänes, A. and Lust, E.
The zero charge potential shift upon adsorption of various organic compounds at bismuth | solution interface, 935
Ehrlich, T., see Ehrlich, J., 935
Eickes, C., Rosenmund, J., Wasle, S., Doblhofer, K., Wang, K. and Weil, K.G.
The electrochemical quartz crystal microbalance (EQCM) in the studies of complex electrochemical reactions, 3623
Eigeldinger, J. and Vogt, H.
The bubble coverage of gas-evolving electrodes in a flowing electrolyte, 4449
Ein-Eli, Y., see Aurbach, D., 67
Eisenblätter, T., see de Alwis, C., 2061
Eiswirth, M., see Zei, M.S., 809
Elizalde, M.P., see Dávila Jiménez, M.M., 4187
Elizalde, M.P., see González, M., 741
Elliott, J.M., see Gollas, B., 3711
El Mouahid, S., see Lamy-Pitara, E., 4299
Endo, A., see Saito, M., 3021
Enyo, M.
Electrochemistry and electrocatalysis research in Japan for on-site power stations and electric vehicles, 4315
Ericson, H., see Mattsson, B., 1405
Ericson, H., Svanberg, C., Brodin, A., Grillone, A.M., Panero, S., Scrosati, B. and Jacobsson, P.
Poly(methyl methacrylate)-based protonic gel electrolytes: a spectroscopic study, 1409
Erné, B.H., see Chazalviel, J.-N., 3205
Ertl, G., see Zei, M.S., 809
Estrany, F., see Brillas, E., 4049
Etchenique, R., see Barbero, C., 3895
Etgens, V.H., Martins Alves, M.C. and Tadjeddine, A.
In situ surface X-ray diffraction studies of electrochemical interfaces at a high-energy third-generation synchrotron facility, 591
Evers, M., see Dakova, B., 4525
Every, H., Bishop, A.G., Forsyth, M. and MacFarlane, D.R.
Ion diffusion in molten salt mixtures, 1279

F

Fabre, P.-L., Dumestre, F., Soula, B. and Galibert, A.-M.
Spectroelectrochemical behaviour in dimethylformamide of pseudo-oxocarbons dianions derived from the croconate dianion, 2697
Fabricius, G., see Bojinov, M., 2029
Fabricius, G., see Bojinov, M., 2791
Fang, S., see Zhang, Z., 2131
Fauvarque, J.-F., see Vassal, N., 1527
Fawcett, W.R., see Hoon-Khosla, M., 611
Fawcett, W.R., see Protsailo, L.V., 3497
Fayolle, F., see Legrand, J., 1791
Fei Wu, J., Che, Y., Okajima, T., Matsumoto, F., Tokuda, K. and Ohsaka, T.
Electroreduction of oxygen in quinoline and isoquinoline, 987
Feliu, J.M., see Climent, V., 629
Fellner, J.P., see Sandhu, S.S., 969
Fermín, D., see Reymond, F., 2647
Fernández, H., see Moressi, M.B., 1669
Ferreira, A.P., see Sottomayor, M.J., 775
Ferry, A., Edman, L., Forsyth, M., MacFarlane, D.R. and Sun, J.
NMR and Raman studies of a novel fast-ion-conducting polymer-in-salt electrolyte based on $LiCF_3SO_3$ and PAN, 1237
Festy, D., see Deslouis, C., 1837
Festy, D., see Herbert-Guillou, D., 1067
Fevrier-Bouvier, A., see Guerin, K., 1607

Fey, G.T.-K. and Huang, D.-L.
Synthesis, characterization and cell performance of inverse spinel electrode materials for lithium secondary batteries, 295
Fieber-Erdmann, M., see Alonso-Vante, N., 4227
Figueiredo, F.M., see Gharbage, B., 2095
Fischer, J.E., see Claye, A., 107
Flandrois, S., see Guerin, K., 1607
Fleischer, G., see Reiche, A., 1327
Florjańczyk, Z., Bzducha, W., Langwald, N., Dygas, J.R., Krok, F. and Misztal-Faraj, B.
Lithium gel polyelectrolytes based on crosslinked maleic anhydride–styrene copolymer, 3563
Florjańczyk, Z., Zygadło-Monikowska, E. and Bzducha, W.
Polymer electrolytes comprising organometallic compounds, 1203
Foresti, M.L., see Forni, F., 3225
Forni, F., Innocenti, M., Pezzatini, G. and Foresti, M.L.
Electrochemical aspects of CdTe growth on the face (111) of silver by ECALE, 3225
Forrest, J.A., see Mattsson, J., 1453
Forsyth, M., Jiazeng, S. and MacFarlane, D.R.
Novel high salt content polymer electrolytes based on high T_g polymers, 1249
Forsyth, M., MacFarlane, D.R. and Hill, A.J.
Glass transition and free volume behaviour of poly(acrylonitrile)/$LiCF_3SO_3$ polymer-in-salt electrolytes compared to poly(ether urethane)/$LiClO_4$ solid polymer electrolytes, 1243
Forsyth, M., see Every, H., 1279
Forsyth, M., see Ferry, A., 1237
Forsyth, M., see McFarlane, D.R., 1271
Fóti, G., see Mousty, C., 451
Fournès, L., see Delmas, C., 243
Franco, G., see Peter, L.M., 549
Frateur, I., see Cattarin, S., 2279
Frichet, A., see Vermoyal, J.J., 1039
Friedrich, K.A., Henglein, F., Stimming, U. and Unkauf, W.
Size dependence of the CO monolayer oxidation on nanosized Pt particles supported on gold, 3283
Fry, A.J., see Carrero, H., 503
Fuchigami, T., see Hou, Y., 3005
Fujimura, K., Matsui, T., Habazaki, H., Kawashima, A., Kumagai, N. and Hashimoto, K.
The durability of manganese–molybdenum oxide anodes for oxygen evolution in seawater electrolysis, 2297
Fujimura, Y., see Senboku, H., 2995
Fujinami, T., Mehta, M.A., Sugie, K. and Mori, K.
Molecular design of inorganic–organic hybrid polyelectrolytes to enhance lithium ion conductivity, 1181
Fujinami, T., see Mehta, M.A., 1175
Fujishima, A., Rao, T.N. and Tryk, D.A.
TiO_2 photocatalysts and diamond electrodes, 4683
Fujishima, A., see Tryk, D.A., 2363
Fujishima, A., see Yoshihara, S., 3375
Funabiki, A., Inaba, M., Abe, T. and Ogumi, Z.
Nucleation and phase-boundary movement upon stage transformation in lithium–graphite intercalation compounds, 865
Funabiki, A., see Inaba, M., 99
Funasaki, N., see Mie, Y., 2903
Furukawa, T., Yoneya, K., Takahashi, Y., Ito, K. and Ohno, H.
Correlation between ionic and dipolar motions in a single-ion conducting polymer P[MEO_9–MAM], 1443
Furuya, N. and Aikawa, H.
Comparative study of oxygen cathodes loaded with Ag and Pt catalysts in chlor-alkali membrane cells, 4251
Fusalba, F. and Bélanger, D.
Electrochemical characterization of polyaniline–molybdenum trisulfide electrode in non-aqueous media, 3877
Fuse, T., Oda, G., Arai, K., Takamura, K. and Kusu, F.
Electrochemical determination of lipase activity in pharmaceutical preparations, 2933
Futerko, P. and Hsing, I.-M.
Two-dimensional finite-element method study of the resistance of membranes in polymer electrolyte fuel cells, 1741

G

Gabrielli, C., see García-Jareño, J.J., 3765
Galibert, A.-M., see Fabre, P.-L., 2697
Galla, U., see Jüttner, K., 2575
Galvele, J.R.
Recent developments in the surface-mobility stress-corrosion-cracking mechanism, 3537
Gamolsky, K., see Levi, M.D., 1781
Gancedo, J.R., see Ríos, E., 4431
Gao, J., see Carrero, H., 503
Gao, X.-P., Sun, Y.-M., Toyoda, E., Higuchi, E., Nakagima, T. and Suda, S.
The effect of the particle pulverization on electrochemical properties of Laves phase alloys, 3099
Gao, Z., see Dai, J., 2211
García Calzón, J.A., see Muñíz Alvarez, J.L., 477
García-Jareño, J.J., Sanmatías, A., Vicente, F., Gabrielli, C., Keddam, M. and Perrot, H.
Study of Prussian Blue (PB) films by ac-electrogravimetry: influence of PB morphology on ions movement, 3765
García-Jareño, J.J., see Sanmatías, A., 797

García-Jareño, J.J., see Trijueque, J., 789
Garrido, J.A., see Benedetti, A.V., 2187
Gauchet, C., see Serpentini, C.-L., 1663
Gautier, J.L., see Ríos, E., 4431
Geoffroy, I., Willmann, P., Mesfar, K., Carré, B. and Lemordant, D.
Electrolytic characteristics of ethylene carbonate–diglyme-based electrolytes for lithium batteries, 2019
Ghanbaja, J., see Naji, A., 1893
Ghanbaja, J., see Thomas, P., 423
Gharbage, B., Figueiredo, F.M., Baker, R.T. and Marques, F.M.B.
Electrochemical permeability of $La_{0.9}Sr_{0.1}Ga_{1-x}Fe_xO_{3-\delta}$, 2095
Giesen, M., Randler, R., Baier, S., Ibach, H. and Kolb, D.M.
Step dynamics on Cu (100) and Ag (111) electrodes in an aqueous electrolyte, 527
Gil, M.L., see Calvente, J.J., 3087
Gil, O., see Deslouis, C., 1837
Gileadi, E., see Daikhin, L., 3615
Gileadi, E., see Zilberman, G., 3473
Giménez, M.C., Del Pópolo, M.G. and Leiva, E.P.M.
Monte Carlo simulation for the formation and growth of low dimensionality phases during underpotential deposition of Ag on Au(100), 699
Ginestar, J., see Serpentini, C.-L., 1663
Ginley, D.S., see McGraw, J.M., 187
Giorgetti, M., Berrettoni, M., Ascone, I., Zamponi, S., Seeber, R. and Marassi, R.
X-ray absorption spectroscopy study on the electrochemical reduction of $Co((DO)(DOH)_{pn})Br_2$, 4475
Giovannelli, G., see Bozzini, B., 3431
Girault, H.H., see Reymond, F., 2647
Girenko, D.V., see Amadelli, R., 713
Girenko, D.V., see Velichenko, A.B., 4341
Glidle, A., Hadyoon, C.S., Cass, A.E.G. and Cooper, J.M.
Modifications of electrodeposited polymers by ion chelation to produce templates for biomolecule immobilisation, 3823
Gojković, S.L., Gupta, S. and Savinell, R.F.
Heat-treated iron(III) tetramethoxyphenyl porphyrin chloride supported on high-area carbon as an electrocatalyst for oxygen reduction: Part III. Detection of hydrogen-peroxide during oxygen reduction, 889
Golding, J., see McFarlane, D.R., 1271
Goldschmidt, M., see Mark, H.B., Jr., 4309
Gollas, B., Elliott, J.M. and Bartlett, P.N.
Electrodeposition and properties of nanostructured platinum films studied by quartz crystal impedance measurements at 10 MHz, 3711
Golodnitsky, D. and Peled, E.
Pyrite as cathode insertion material in rechargeable lithium/composite polymer electrolyle batteries, 335
Golodnitsky, D. and Peled, E.
Stretching-induced conductivity enhancement of LiI–(PEO)-polymer electrolyte, 1431
Golodnitsky, D., see Strauss, E., 1519
Gomathi, H., see Vittal, R., 2083
Gomes, J.A.N.F., see Gomes, J.R.B., 653
Gomes, J.A.N.F., see Ignaczak, A., 659
Gomes, J.R.B. and Gomes, J.A.N.F.
A DFT study of dioxymethylene adsorption on the copper (111) surface, 653
Gómez, R., see Climent, V., 629
Gong, J. and Wu, H.
Electrochemical intercalation of lithium species into disordered carbon prepared by the heat-treatment of poly (*p*-phenylene) at 650°C for anode in lithium-ion battery, 1753
González, I., see Cisneros-González, I., 2729
González, J., see Abrantes, L.M., 457
González, J., see Molina, A., 761
González, M., Elizalde, M.P., Baños, L., Poillerat, G. and Dávila, M.M.
Surface characterization of $LaNiO_3$/Ni–PVC composite, 741
González, M., see Dávila Jiménez, M.M., 4187
González-Tejera, M.J., Carrillo Ramiro, I. and Hernández-Fuentes, I.
Nucleation and growth mechanism of polyfurane perchlorate doped films, 1973
Goto, T., Obata, R. and Ito, Y.
Electrochemical formation of iron nitride film in a molten LiCl–KCl–Li_3N system, 3367
Goto, T., see Abe, T., 4009
Govindaraj, A., see Rajalakshmi, N., 4511
Grabec-Švegl, I., see Švegl, F., 4359
Greenbaum, S.G., see Ratnakumar, B.V., 1513
Grigor'ev, V., see Guterman, V., 873
Grillone, A.M., see Ericson, H., 1409
Groult, H., see Lantelme, F., 3171
Grundmeier, G., Schmidt, W. and Stratmann, M.
Corrosion protection by organic coatings: electrochemical mechanism and novel methods of investigation, 2515
Grüne, M., see Delmas, C., 243
Grygar, T., see Bezdička, P., 913
Grzeszczuk, M. and Poks, P.
The HER performance of colloidal Pt nanoparticles incorporated in polyaniline, 4171
Guascito, M.R., see Casella, I.G., 1113
Gu, G.Y., Bouvier, S., Wu, C., Laura, R., Rzeznik, M. and Abraham, K.M.
2-Methoxyethyl (methyl) carbonate-based electrolytes for Li-ion batteries, 3127
Gu, H.-B., Kim, J.-U., Song, H.-W., Park, G.-C. and Park, B.-K.

Electrochemical properties of carbon composite electrode with polymer electrolyte for electric double-layer capacitor, 1533
Gu, Z., see Liu, T., 2743
Gu, Z., see Liu, T., 4457
Gu, Z., see Wei, M., 4441
Guel, B., see Krumm, R., 3255
Guerin, K., Fevrier-Bouvier, A., Flandrois, S., Simon, B. and Biensan, P.
On the irreversible capacities of disordered carbons in lithium-ion rechargeable batteries, 1607
Guerriero, P., see Cattarin, S., 2279
Guidelli, R. and Schmickler, W.
Recent developments in models for the interface between a metal and an aqueous solution, 2317
Guilerez, S., see Barth, M., 4409
Gupta, S., see Gojković, S.L., 889
Gupta, V., see Nakajima, T., 1655
Guterman, V., Averina, Y. and Grigor'ev, V.
The effect of the composition of aluminum alloys on electrochemical incorporation of lithium, 873
Guyomard, D., see Potiron, E., 197

H

Haarberg, G.M., see Kjelstrup, S., 2707
Haas, O., see Novák, P., 351
Habazaki, H., see Fujimura, K., 2297
Habazaki, H., see Shimizu, K., 1805
Hadyoon, C.S., see Glidle, A., 3823
Hagenström, H., Schneeweiss, M.A. and Kolb, D.M.
Copper underpotential deposition on ethanethiol-modified Au(111) electrodes: kinetic effects, 1141
Haiss, W., see Raisch, P., 4635
Hall, S.B., Khudaish, E.A. and Hart, A.L.
Electrochemical oxidation of hydrogen peroxide at platinum electrodes. Part V: inhibition by chloride, 3573
Hammou, A., see Vermoyal, J.J., 1039
Hamnett, A., see Christensen, P., 2443
Hamnett, A., see Reeve, R.W., 4237
Handel, H., see Simon, E., 855
Han, J.-N. and Pyun, S.-I.
Analysis of open-circuit potential transient and laser beam deflection transient simultaneously measured from Pd foil electrode pre-charged with hydrogen, 2781
Han, S. and Lindholm-Sethson, B.
Electrochemistry at ultrathin polyelectrolyte films self-assembled at planar gold electrodes, 845
Hara, K., see Tsuruhara, K., 1223
Harima, Y., see Tang, H., 2771
Harima, Y., see Zhu, L., 2203
Hart, A.L., see Hall, S.B., 3573
Hashimoto, K., see Fujimura, K., 2297
Hashimoto, K., see Yoshihara, S., 3375
Hasoň, S., see Vetterl, V., 2961
Hassel, A.W., Aihara, M. and Seo, M.
Formation and corrosion of InP/In contacts in hydrochloric acid, 4673
Hatton, R., see Zeng, X., 3629
Hauptmann, P., see Lucklum, R., 3907
Hawkridge, F.M., see Rhoten, M.C., 2855
Hay, R.W., see de Alwis, C., 2061
Hayamizu, K., Aihara, Y., Arai, S. and Price, W.S.
Self-diffusion coefficients of lithium, anion, polymer, and solvent in polymer gel electrolytes measured using ^{7}Li, ^{19}F, and ^{1}H pulsed-gradient spin-echo NMR, 1313
Hayamizu, K., see Aihara, Y., 1321
He, D., see Zhou, A., 3943
Heider, U., see Levi, M.D., 1781
Heinze, J., see Hess, C., 3725
Henderson, M.J., Hillman, A.R. and Vieil, E.
Chronoamperometric resolution of ion and solvent transfers at a poly(*o*-toluidine) modified electrode by combined electrochemical quartz crystal microbalance (EQCM) and probe beam deflection (PBD), 3885
Henglein, F., see Friedrich, K.A., 3283
Henrion, O., see Beerbom, M., 4663
Henry de Villeneuve, C., see Allongue, P., 3241
Henry de Villeneuve, C., see Allongue, P., 4591
Hepel, M. and Janusz, W.
Study of leuco-methylene blue film growth and its reoxidation on sulphur-modified Au-EQCN electrode, 3785
Herbert-Guillou, D., Tribollet, B., Festy, D. and Kiéné, L.
In situ detection and characterization of biofilm in waters by electrochemical methods, 1067
Hernández-Fuentes, I., see González-Tejera, M.J., 1973
Hess, C., Borgwarth, K. and Heinze, J.
Integration of an electrochemical quartz crystal microbalance into a scanning electrochemical microscope for mechanistic studies of surface patterning reactions, 3725
Hickey, S.G. and Riley, D.J.
Intensity modulated photocurrent spectroscopy studies of CdS nanoparticle modified electrodes, 3277
Hiesgen, R., Krause, M. and Meissner, D.
STM measurement of current–potential curves at a semiconductor surface, 3213
Higashiya, S., see Hou, Y., 3005
Higuchi, E., see Gao, X.-P., 3099
Higuchi, E., see Li, Z.P., 1773
Hill, A.J., see Forsyth, M., 1243
Hillman, A.R., see Bruckenstein, S., 3801
Hillman, A.R., see Henderson, M.J., 3885
Hinken, J.H., see Juzeliúnas, E., 3453

Hirao, M., Ito, K. and Ohno, H.
Preparation and polymerization of new organic molten salts; *N*-alkylimidazolium salt derivatives, 1291
Hirata, Y., Mizutani, F. and Yokoyama, H.
Microscopic detection of light-induced electron transfer in molecular assembly system using scanning Maxwell stress microscopy (SMM), 2953
Hirose, T., see Okada, T., 4419
Hjuler, H.A., see Qingfeng, L., 4219
Holub-Krappe, E., see Alonso-Vante, N., 4227
Holze, R., see Bron, M., 1121
Honda, K., see Tryk, D.A., 2363
Honeycutt, L., see Le Granvalet-Mancini, M., 1491
Hoon-Khosla, M., Fawcett, W.R., Chen, A., Lipkowski, J. and Pettinger, B.
A SNIFTIRS study of the adsorption of pyridine at the Au(111) electrode–solution interface, 611
Horgan, M.A., see Burke, L.D., 4127
Hori, Y., see Hoshi, N., 4263
Hoshi, N. and Hori, Y.
Electrochemical reduction of carbon dioxide at a series of platinum single crystal electrodes, 4263
Hou, Y., Higashiya, S. and Fuchigami, T.
Electrolytic partial fluorination of organic compounds. Part 34. Regioselective anodic fluorination of benzyl thiocyanate and its derivatives, 3005
Howells, W.S., see Carlsson, P., 1449
Hsing, I.-M., see Futerko, P., 1741
Hu, C.-C. and Chang, K.-H.
Cyclic voltammetric deposition of hydrous ruthenium oxide for electrochemical capacitors: effects of codepositing iridium oxide, 2685
Hu, C.-C. and Liu, K.-Y.
Voltammetric investigation of platinum oxides II. Effect of hydration on their reduction behavior, 3063
Huang, C.K., see Ratnakumar, B.V., 1513
Huang, D.-L., see Fey, G.T.-K., 295
Huang, H.G., see Wu, L.L., 2877
Huerta, F.J., see Quijada, C., 1847
Huerta, F., see Montilla, F., 4271
Hui, K.C.A., see Wilde, C.P., 3649
Hurley, L.M., see Burke, L.D., 4127
Hwang, H.-Y., see Song, H.-K., 2241

I

Ibach, H., see Giesen, M., 527
Ibach, H.
Stress in densely packed adsorbate layers and stress at the solid–liquid interface — is the stress due to repulsive interactions between the adsorbed species?, 575
Idla, K., Inganäs, O. and Strandberg, M.
Good adhesion between chemically oxidised titanium and electrochemically deposited polypyrrole, 2121
Ignaczak, A., Gomes, J.A.N.F. and Cordeiro, M.N.D.S.
Quantum and simulation studies of $X^-(H_2O)_n$ systems, 659
Iijima, S., see Mizutani, F., 2945
Ikeda, T., see Ogata, Y.H., 2219
Ikeda, Y., Wada, Y., Matoba, Y., Murakami, S. and Kohjiya, S.
Characterization of comb-shaped high molecular weight poly(oxyethylene) with tri(oxyethylene) side chains for a polymer solid electrolyte, 1167
Ikezawa, Y., Koda, Y., Shibuya, M. and Terashima, H.
In situ FTIR study of pyrazine adsorbed on Au(111), Au(100) and Au(110) electrodes, 2075
Ikezawa, Y., Sekiguchi, R. and Kitazume, T.
Adsorption of benzoic acid on an Au (100) electrode in acidic media by IRAS, 1089
Illas, F., see Curulla, D., 639
Imae, I., see Ohsedo, Y., 1543
Imanishi, A., see Zhou, X., 4655
Imhof, R., see Novák, P., 351
Inaba, M., Kawatate, Y., Funabiki, A., Jeong, S.-K., Abe, T. and Ogumi, Z., 99
Inaba, M., see Funabiki, A., 865
Inaba, M., see Maruyama, J., 415
Inganäs, O., see Idla, K., 2121
Ingram, M., see Depre, L., 1377
Innocenti, M., see Forni, F., 3225
Inoue, H., see Yoshida, Y., 409
Inoue, S., see Mehta, M.A., 1175
Inoue, T., see Mehta, M.A., 1175
Inzelt, G.
Simultaneous chronoamperometric and quartz crystal microbalance studies of redox transformations of polyaniline films, 3865
Inzelt, G., Pineri, M., Schultze, J.W. and Vorotyntsev, M.A.
Electron and proton conducting polymers: recent developments and prospects, 2403
Ishida, M., see Zhou, X., 4655
Ishikawa, M., see Morita, M., 1335
Ishikawa, M., see Yamada, O., 2197
Ishiko, E., see Kono, M., 1307
Ito, K., Nishina, N. and Ohno, H.
Enhanced ion conduction in imidazolium-type molten salts, 1295
Ito, K., see Furukawa, T., 1443
Ito, K., see Hirao, M., 1291
Ito, Y. and Nohira, T.
Non-conventional electrolytes for electrochemical applications, 2611

Ito, Y., see Goto, T., 3367
Ito-Akita, K., see Yoshizawa, M., 1617
Itoh, K., see Nishiguchi, I., 2991
Iwahori, T., Mitsuishi, I., Shiraga, S., Nakajima, N., Momose, H., Ozaki, Y., Taniguchi, S., Awata, H., Ono, T. and Takeuchi, K.
Development of lithium ion and lithium polymer batteries for electric vehicle and home-use load leveling system application, 1509
Iwakura, C., see Yoshida, Y., 409
Izuchi, S., see Murata, K., 1501

J

Jacob, K.T., Okabe, T.H., Uda, T. and Waseda, Y.
Solid-state cells with buffer electrodes for accurate thermodynamic measurements: system Nd–Ir–O, 1963
Jacob, M.M.E. and Arof, A.K.
FTIR studies of DMF plasticized polyvinyledene fluoride based polymer electrolytes, 1701
Jacobsson, P., see Carlsson, P., 1449
Jacobsson, P., see Ericson, H., 1409
Jaegermann, W., see Beerbom, M., 4663
Jakšić, J.M., Vojnović, M.V. and Krstajić, N.V.
Kinetic analysis of hydrogen evolution at Ni–Mo alloy electrodes, 4151
Jakšić, M.M.
Hypo–hyper-*d*-electronic interactive nature of synergism in catalysis and electrocatalysis for hydrogen reactions, 4085
Jakšić, M.M., see Ristic, N.M., 2973
Jänes, A., see Ehrlich, J., 935
Janik-Czachor, M., Szummer, A., Molnar, A., Dolata, M., Kudelski, A., Varga, M., Bukowska, J. and Sikorski, K.
Electrochemical modification of Cu–Zr amorphous alloys for catalysts, 3295
Janowitz, K., Kah, M. and Wendt, H.
Molten carbonate fuel cell research: Part I. Comparing cathodic oxygen reduction in lithium/potassium and lithium/sodium carbonate melts, 1025
Jansen, A.P.J., see Koper, M.T.M., 645
Janusz, W., see Hepel, M., 3785
Jasulaitiene, V., see Zalewska, T., 4031
Jeong, S.-K., see Inaba, M., 99
Jerkiewicz, G., see Conway, B.E., 4075
Jeziorek, D., see Ossowski, T., 3581
Jiang, J. and Kucernak, A.
The electrochemistry of platinum phthalocyanine microcrystals: I. Electrochemical behaviour in acetonitrile electrolytes, 2227
Jiang, R. and Chu, D.
Multiple small potential steps at a rotating disk electrode and applications, 4025
Jiazeng, S., see Forsyth, M., 1249
Joachin, H., see Prakash, J., 2289
Johannsen, K., Page, D. and Roy, S.
A systematic investigation of current efficiency during brass deposition from a pyrophosphate electrolyte using RDE, RCE, and QCM, 3691
Johansson, P., Tegenfeldt, J. and Lindgren, J.
Conformational analysis of a model of the sidechains in perfluorosulfonated membranes, 3055
John, S.A. and Ohsaka, T.
Stabilization of the assemblies of short alkyl chain asymmetric viologens on alkanethiol-coated electrodes, 1127
John, S.A., Kitamura, F., Tokuda, K. and Ohsaka, T.
Can *N*-ethyl-*N'*-octadecyl viologen dimerize on octadecanethiol-coated gold electrode ?, 4041
Joho, F. and Novák, P.
SNIFTIRS investigation of the oxidative decomposition of organic-carbonate-based electrolytes for lithium-ion cells, 3589
Jokic, A.M., see Ristic, N.M., 2973
Jouikov, V.
Bimolecular reactions of electrogenerated cation radicals of arylmethylselenides, 3939
Jouikov, V., Biran, C., Bordeau, M. and Dunoguès, J.
Homogeneous redox catalysed reduction of chloromethyldimethylchlorosilane, 1015
Jovanic, B., see Belca, I., 993
Jovanic, B., see Belca, I.D., 4059
Jukić, A., see Metikoš-Huković, M., 977
Jukić, A., see Metikoš-Huković, M., 4159
Jungblut, H., see Lewerenz, H.J., 4615
Jusys, Z. and Stalnionis, G.
Wall-jet electrochemical quartz crystal microgravimetry: oxidation of Co(II)–ethylenediamine complexes on copper electrode, 3675
Jüttner, K., Galla, U. and Schmieder, H.
Electrochemical approaches to environmental problems in the process industry, 2575
Juzeliúnas, E. and Hinken, J.H.
A SQUID study of magnetic fields induced by the metal–liquid interface, 3453

K

Kageyama, H., see Capiglia, C., 1341
Kageyama, H., see Kawai, H., 315
Kah, M., see Janowitz, K., 1025
Kaiser, W., see Beck, F., 4691
Kálmán, E., see Telegdi, J., 3639
Kamekawa, H., see Senboku, H., 2995
Kamiyama, T., see Yasuda, Y., 1537
Kaneko, M., see Abe, T., 4009
Kaneko, M., see Zhang, J., 399

Kang, S.K., Chung, T.D. and Kim, H.
Electrochemical recognition of Ca^{2+} ion in basic aqueous media using quinone-derivatized calix[4]arene, 2939
Kankare, J., see Visy, C., 1811
Kankare, J., see Visy, C., 3851
Kanno, H., see Naoi, K., 3413
Kanno, H., see Suematsu, S., 3813
Karmann, E., see Schlettwein, D., 4697
Kasalica, B., see Belca, I., 993
Kashiwamura, K., see Morita, M., 1335
Kasuga, K., see Okada, T., 4419
Kato, M., see Tsuruhara, K., 1391
Kaučič, V., see Švegl, F., 4359
Kawahara, M., Morita, J., Rikukawa, M., Sanui, K. and Ogata, N.
Synthesis and proton conductivity of thermally stable polymer electrolyte: poly(benzimidazole) complexes with strong acid molecules, 1395
Kawahara, M., see Tsuruhara, K., 1223
Kawai, H., Nagata, M., Kageyama, H., Tukamoto, H. and West, A.R., 315
Kawashima, A., see Fujimura, K., 2297
Kawatate, Y., see Inaba, M., 99
Keddam, M., see García-Jareño, J.J., 3765
Kelly, J.J., Kooij, E.S. and Meulenkamp, E.A.
Luminescence studies of semiconductor electrodes, 561
Kelly, J.J., see Xia, X.H., 4645
Kelsall, G.H., see Kucernak, A.R., 4483
Kemell, M., Saloniemi, H., Ritala, M. and Leskelä, M.
Electrochemical quartz crystal microbalance study of the electrodeposition mechanisms of $Cu_{2-x}Se$ thin films, 3737
Kertesz, V., Chambers, J.Q. and Mullenix, A.N.
Chronoamperometry of surface-confined redox couples. Application to daunomycin adsorbed on hanging mercury drop electrodes, 1095
Kharkats, Y.I., see Nazmutdinov, R.R., 3521
Khudaish, E.A., see Hall, S.B., 3573
Kiéné, L., see Herbert-Guillou, D., 1067
Kikawa, K., see Yoshida, Y., 409
Kim, C.-K., see Cho, E.-A., 1933
Kim, C.S. and Oh, S.M.
Importance of donor number in determining solvating ability of polymers and transport properties in gel-type polymer electrolytes, 2101
Kim, H., see Kang, S.K., 2939
Kim, H., see Min, M.-k., 4211
Kim, H.-S., Nishizawa, M. and Uchida, I.
Single particle electrochemistry for hydrogen storage alloys, $MmNi_{3.55}Co_{0.75}Mn_{0.4}Al_{0.3}$, 483
Kim, H.-T., Kim, K.-B., Kim, S.-W. and Park, J.-K.
Li-ion polymer battery based on phase-separated gel polymer electrolyte, 4001
Kim, J.-S., see Cho, E.-A., 1933
Kim, J.-U., see Gu, H.-B., 1533
Kim, K.-B., see Kim, H.-T., 4001
Kim, S.H., Lee, J.W. and Yeo, I.-H.
Spectroelectrochemical and electrochemical behavior of epinephrine at a gold electrode, 2889
Kim, S., see Myung, N., 3749
Kim, S.-W., see Kim, H.-T., 4001
Kim, W.-J., see Lee, K.-H., 1301
Kim, Y., see Paik, W., 3833
Kim, Y., Teshima, K. and Kobayashi, N.
Improvement of reversible photoelectrochromic reaction of polyaniline in polyelectrolyte composite film with the dichloroethane solution system, 1549
Kim, Y.W., Lee, W. and Choi, B.K.
Relation between glass transition and melting of PEO–salt complexes, 1473
Kim, Y.W., see Choi, B.K., 1371
Kinnunen, P., see Bojinov, M., 2791
Kishita, M., see Mie, Y., 2903
Kitamura, F., see John, S.A., 4041
Kitani, A., see Zhu, L., 2203
Kitazume, T., see Ikezawa, Y., 1089
Kjelstrup, S., Qian, J. and Haarberg, G.M.
The Peltier heating of the aluminium cathode in contact with cryolite–alumina melts, 2707
Klápště, B., see Bezdička, P., 913
Klein, A., see Beerbom, M., 4663
Klintenberg, M., see Aabloo, A., 1425
Kobayashi, N., see Kim, Y., 1549
Kobayashi, S.-i., see Taniguchi, I., 2843
Kobayashi, T., see Ogata, Y.H., 2219
Kocha, S.S., see Aroutiounian, V.M., 1999
Koda, Y., see Ikezawa, Y., 2075
Koenig, J.-F., see Singh, R.N., 1911
Koh, M., see Nakajima, T., 1655
Kohjiya, S., see Ikeda, Y., 1167
Koksbang, R., see West, K., 3141
Kolb, D.M.
Structure studies of metal electrodes by in-situ scanning tunneling microscopy, 2387
Kolb, D.M., see Giesen, M., 527
Kolb, D.M., see Hagenström, H., 1141
Kolb, D.M., see Ziegler, J.C., 827
Kolb, D.M., see Ziegler, J.C., 4599
Kolodziej-Sadlok, M., see Zak, J., 2803
Kondratiev, V.V., Tikhomirova, A.V. and Malev, V.V.
Study of charge transport processes in Prussian-blue film modified electrodes, 751
Kong, F., see Kostecki, R., 225
Kono, M., Nishiura, M., Ishiko, E. and Sada, T.
Novel gel polymer electrolytes based on alkylene oxide macromonomer, 1307
Kooij, E.S., see Kelly, J.J., 561
Koper, M.T.M., Jansen, A.P.J. and Lukkien, J.J.
Lattice–gas modeling of electrochemical Langmuir–Hinshelwood surface reactions, 645
Kornyshev, A.A., see Daikhin, L.I., 685

Kostecki, R., Kong, F., Matsuo, Y. and McLarnon, F.
Interfacial studies of a thin-film $Li_2Mn_4O_9$ electrode, 225
Kotorcevic, M., see Ristic, N.M., 2973
Kötz, R. and Carlen, M.
Principles and applications of electrochemical capacitors, 2483
Koudelka-Hep, M. and van der Wal, P.D.
Microelectrode sensors for biomedical and environmental applications, 2437
Kovalyov, S.V., see Amadelli, R., 713
Kramer, S., see Scott, K., 945
Krause, M., see Hiesgen, R., 3213
Krestyn, E., see Mie, Y., 2903
Kriván, E., see Visy, C., 3851
Krohn, H., see Beck, F., 4691
Krok, F., see Florjańczyk, Z., 3563
Krotine, J., see Mark, H.B., Jr., 4309
Krozer, A., see Mattsson, J., 1453
Krstajić, N.V., see Jakšić, J.M., 4151
Krumm, R., Guel, B., Schmitz, C. and Staikov, G.
Nucleation and growth in electrodeposition of metals on n-Si(111), 3255
Krysinski, P., Moncelli, M.R. and Tadini-Buoninsegni, F.
A voltammetric study of monolayers and bilayers self-assembled on metal electrodes, 1885
Kubo, K., see Tanaka, R., 1385
Kucernak, A.R., Chowdhury, P.B., Wilde, C.P., Kelsall, G.H., Zhu, Y.Y. and Williams, D.E.
Scanning electrochemical microscopy of a fuel-cell electrocatalyst deposited onto highly oriented pyrolytic graphite, 4483
Kucernak, A., see Jiang, J., 2227
Kudelski, A., see Janik-Czachor, M., 3295
Kudryavtseva, Z.I., see Pshenichnikov, A.G., 4143
Kuhn, A., see Martel, D., 1829
Kulak, A.I., see Poznyak, S.K., 1595
Kulandaisamy, S., Rethinaraj, J.P., Chockalingam, S.C., Venkateswaran, K.V. and Visvanathan, S.
Spinel oxide coated titanium anodes–preparation and characterization, 3047
Kulesza, P.J., see Malik, M.A., 3777
Kumagai, N., see Fujimura, K., 2297
Kumagai, N., see Lantelme, F., 3171
Kunai, A., see Tang, H., 2771
Kunai, A., see Zhu, L., 2203
Kunugi, Y., see Tang, H., 2771
Kunugi, Y., see Zhu, L., 2203
Kurusu, F. and Ohno, H.
Long-term stability of conformation and redox response of cross-linked cytochrome *c* in polymer solvent, 2911
Kusu, F., see Arai, K., 3029
Kusu, F., see Fuse, T., 2933
Kuwabata, S., see Torimoto, T., 3269
Kuznetsov, A.M. and Ulstrup, J.
Theory of electron transfer at electrified interfaces, 2339
Kuznetsov, A.M., see Nazmutdinov, R.R., 3521
Kwon, H.-S., see Cho, E.-A., 1933

L

Lacaze, P.-C., see Sakmeche, N., 1921
Lacnjevac, C.M., see Ristic, N.M., 2973
Laitinen, T., see Bojinov, M., 2029
Laitinen, T., see Bojinov, M., 2791
Lakshminarayanan, V., see Subramanian, R., 4501
Lal, B., see Singh, R.N., 1911
Lampeka, Y.D., see de Alwis, C., 2061
Lamy-Pitara, E., El Mouahid, S. and Barbier, J.
Effect of anions on catalytic and electrocatalytic hydrogenations and on the electrocatalytic oxidation and evolution of hydrogen on platinum, 4299
Lamy-Pitara, E., see Quiroz, M.A., 4291
Landolt, D., see Bradley, P.E., 1077
Landolt, D., see Datta, M., 2535
Landolt, D., see Schmutz, P., 899
Landolt, D., see Zech, N., 3461
Lane, D.W., see Duffy, N.W., 3355
Langwald, N., see Florjańczyk, Z., 3563
Lantelme, F., Groult, H. and Kumagai, N.
Study of the concentration-dependent diffusion in lithium batteries, 3171
Łapkowski, M., see Barth, M., 4409
Laura, R., see Gu, G.Y., 3127
Lavela, P., see Bach, S., 931
Lee, C.-W., see Carrero, H., 503
Lee, H.J., see Reymond, F., 2647
Lee, J.-S., see Shim, J., 1943
Lee, J.W., see Kim, S.H., 2889
Lee, K.-H., Park, J.-K. and Kim, W.-J.
Electrochemical characteristics of PAN ionomer based polymer electrolytes, 1301
Lee, K.-H., see Song, H.-K., 2241
Lee, W., see Kim, Y.W., 1473
Lee, W.-J. and Pyun, S.-I.
Effects of sulphate ion additives on the pitting corrosion of pure aluminium in 0.01 M NaCl solution, 1901
Le Gal La Salle, A., see Potiron, E., 197
Legrand, J., Dumont, E., Comiti, J. and Fayolle, F.
Diffusion coefficients of ferricyanide ions in polymeric solutions — comparison of different experimental methods, 1791
Le Granvalet-Mancini, M., Honeycutt, L. and Teeters, D.
Characterization of self-assembled molecular layers at the polymer electrolyte/lithium electrode interface, 1491

Leiva, E.P.M., see Giménez, M.C., 699
Leiva, E.P.M., see Sánchez, C., 691
Lemordant, D., see Geoffroy, I., 2019
Lepiller, C., see Myung, N., 3749
Le Rille, A., see Tadjeddine, A., 601
Leskelä, M., see Kemell, M., 3737
Leventis, N., see Collins, C.M., 2049
Levi, E., see Aurbach, D., 67
Levi, M.D. and Aurbach, D.
Frumkin intercalation isotherm — a tool for the description of lithium into host materials: a review, 167
Levi, M.D., Gamolsky, K., Aurbach, D., Heider, U. and Oesten, R.
On electrochemical impedance measurements of $Li_xCo_{0.2}Ni_{0.8}O_2$ and Li_xNiO_2 intercalation electrodes, 1781
Lewerenz, H.J., Jungblut, H. and Rauscher, S.
Surface analysis of the electropolishing layer on Si(111) in ammonium fluoride solution, 4615
Lezna, R.O., see Borrás, C.A., 1717
Lezna, R.O., see de Tacconi, N.R., 3403
L'Her, M., see Simon, E., 855
Lhotský, A., see Samec, Z., 583
Li, C.-z., Nishiyama, K. and Taniguchi, I.
Electrochemical and spectroelectrochemical studies on cobalt myoglobin, 2883
Li, J.X., see Wu, L.L., 2877
Li, M., see Liu, T., 2743
Li, M., see Liu, T., 4457
Li, N., see Liu, T., 2743
Li, N., see Liu, T., 4457
Li, N., see Wei, M., 4441
Li, S.F.Y., see Dai, J., 2211
Li, X.-y., see Pei, J., 1581
Li, Y. and Qian, R.
Electrochemical overoxidation of conducting polypyrrole nitrate film in aqueous solutions, 1727
Li, Z.P., Higuchi, E., Liu, B.H. and Suda, S.
Effects of fluorination temperature on surface structure and electrochemical properties of AB_2 electrode alloys, 1773
Liao, C.-M. and Wei, R.P.
Galvanic coupling of model alloys to aluminum — a foundation for understanding particle-induced pitting in aluminum alloys, 881
Lin, H.C., see Yan, C.W., 2815
Lin, Z., see Wu, L., 2923
Lin, Z.H., see Wu, L.L., 2877
Lincot, D., see Myung, N., 3749
Lincot, D., see Pauporté, T., 3345
Lindgren, J., see Johansson, P., 3055
Lindgren, J., see Ludvigsson, M., 2267
Lindholm-Sethson, B., see Han, S., 845
Lipkowski, J., see Hoon-Khosla, M., 611
Lisowska-Oleksiak, A., see Zalewska, T., 4031
Liu, B.H., see Li, Z.P., 1773
Liu, B., see Liu, S., 1683
Liu, K.-Y., see Hu, C.-C., 3063
Liu, P., Yang, Q., Tong, Y. and Yang, Y.
Electrodeposition of Gd–Co film in organic bath, 2147
Liu, S., Wang, B., Liu, B. and Dong, S.
Electrochemical behavior of redox species at carbon fibre microdisk array electrode modified with mixed-valent molybdenum(VI, V) oxide, 1683
Liu, T., Li, M., Li, N., Gu, Z. and Zhou, X.
Electrocatalytic reduction of halogenated acid at electrodes chemically modified with C_{60}-octasodium calix[8]aryloxy octakis-(propane-3-sulphonate) complex and Nafion films, 4457
Liu, T., Li, M., Li, N., Shi, Z., Gu, Z. and Zhou, X.
Voltammetric behavior of C_{60}-octasodium calix[8]aryloxy octakis-(propane-3-sulphonate) complex and Nafion films, 2743
Liu, Y., see Song, W., 1639
Liwo, A., see Ossowski, T., 3581
Lohrengel, M.M., see Schultze, J.W., 2499
López Fonseca, J.M., see Muñíz Alvarez, J.L., 477
Lorenz, W.J., see Budevski, E., 2559
Lu, N., see Song, W., 1639
Lucklum, R. and Hauptmann, P.
The Δf–ΔR QCM technique: an approach to an advanced sensor signal interpretation, 3907
Ludvigsson, M., Lindgren, J. and Tegenfeldt, J.
FTIR study of water in cast Nafion films, 2267
Lukkien, J.J., see Koper, M.T.M., 645
Luo, J.L., see Cheng, Y.F., 1763
Luo, J.L., see Cui, N., 3973
Luo, J.L., see Yang, Q., 3927
Luo, J., see Wu, L., 2923
Luo, J., see Wu, L.L., 2877
Lust, E., see Ehrlich, J., 935
Lust, E., see Lust, K., 3543
Lust, E., see Väärtnõu, M., 1623
Lust, K., Väärtnõu, M. and Lust, E.
Adsorption of halide anions on bismuth single crystal plane electrodes, 3543
Lutar, K., see Nakajima, T., 1655

M

Macdonald, D.D., see Sikora, J., 1875
MacFarlane, D.R., see Every, H., 1279
MacFarlane, D.R., see Ferry, A., 1237
MacFarlane, D.R., see Forsyth, M., 1249
MacFarlane, D.R., see Forsyth, M., 1243
Machado, S.A.S., see Correia, A.N., 1733
Machado, S.A.S., see de Oliveira-Sousa, A., 4467
Maekawa, H., see Nishiguchi, I., 2991
Maffi, S., see Decker, F., 4607
Maillot, V., see Deslouis, C., 1837

Mäkelä, K., see Bojinov, M., 2029
Mäkelä, K., see Bojinov, M., 2791
Maki, T., see Matsumura, Y., 3011
Malev, V.V., see Kondratiev, V.V., 751
Malik, M.A., Miecznikowski, K. and Kulesza, P.J.
Quartz crystal microbalance monitoring of mass transport during redox processes of cyanometallate modified electrodes: complex charge transport in nickel hexacyanoferrate films, 3777
Mandler, D., see Muskal, N., 537
Marassi, R., see Appetecchi, G.B., 23
Marassi, R., see Giorgetti, M., 4475
Marco, J.F., see Ríos, E., 4431
Mareček, V., see Samec, Z., 583
Mark, H.B., Jr., Rubinson, J.F., Krotine, J., Vaughn, W. and Goldschmidt, M.
Catalysis of the reduction of acetylene at poly-3-methylthiophene electrodes, 4309
Marković, N.M. and Ross, P.N.
Electrocatalysts by design: from the tailored surface to a commercial catalyst, 4101
Markovsky, B., see Aurbach, D., 67
Maroun, F., see Chazalviel, J.-N., 3205
Marozzi, C.A. and Chialvo, A.C.
Development of electrode morphologies of interest in electrocatalysis. Part 1: Electrodeposited porous nickel electrodes, 2111
Marques, F.M.B., see Gharbage, B., 2095
Martel, D. and Kuhn, A.
Electrocatalytic reduction of H_2O_2 at $P_2Mo_{18}O_{62}^{6-}$ modified glassy carbon, 1829
Martens, T., see Dakova, B., 4525
Martins Alves, M.C., see Etgens, V.H., 591
Martinez-Ortiz, F., Alcaraz, M.-L. and Roca, I.
New developments in cyclic voltammetry at the dropping mercury electrode, 387
Maruyama, J., Inaba, M. and Ogumi, Z.
Effect of fluorinated alcohol on the kinetics of cathodic oxygen reduction at gold electrodes, 415
Mastragostino, M., see Arbizzani, C., 2273
Matoba, Y., see Ikeda, Y., 1167
Matsubara, T., see Morimoto, T., 4257
Matsui, T., see Fujimura, K., 2297
Matsumoto, F., see Fei Wu, J., 987
Matsumura, Y., Satoh, Y., Maki, T. and Onomura, O.
The electrochemically induced Hofmann rearrangement and its comparison with the classic Hofmann rearrangement, 3011
Matsunaga, T., see Okochi, M., 2917
Matsuo, Y., see Kostecki, R., 225
Matsushita, K., see Mehta, M.A., 1175
Mattsson, B., Ericson, H., Torell, L.M. and Sundholm, F.
Degradation of a fuel cell membrane, as revealed by micro-Raman spectroscopy, 1405
Mattsson, J., Forrest, J.A., Krozer, A., Södervall, U., Wennerberg, A. and Torell, L.M.
Characterisation of sub micron salt-doped polymer electrolyte films, 1453
Mayer, T., see Beerbom, M., 4663
McFarlane, D.R., Sun, J., Golding, J., Meakin, P. and Forsyth, M.
High conductivity molten salts based on the imide ion, 1271
McGraw, J.M., Bahn, C.S., Parilla, P.A., Perkins, J.D., Readey, D.W. and Ginley, D.S.
Li ion diffusion measurements in V_2O_5 and $Li(Co_{1-x}Al_x)O_2$ thin-film battery cathodes, 187
McGreevy, R.L., see Carlsson, P., 1449
McLarnon, F., see Kostecki, R., 225
McMurray, H.N., see Böhm, S., 2165
Meakin, P., see McFarlane, D.R., 1271
Medina, J., see Barrado, E., 1105
Mehta, M.A., Fujinami, T., Inoue, S., Matsushita, K., Miwa, T. and Inoue, T.
The use of boroxine rings for the development of high performance polymer electrolytes, 1175
Mehta, M.A., see Fujinami, T., 1181
Meier, A., see Siemoneit, K., 4577
Meissner, D., see Hiesgen, R., 3213
Mellander, B.-E., see Vargas, M.A., 1399
Memming, R., see Siemoneit, K., 4577
Ménétrier, M., see Delmas, C., 243
Mesfar, K., see Geoffroy, I., 2019
Metikoš-Huković, M. and Jukić, A.
Correlation of electronic structure and catalytic activity of Zr–Ni amorphous alloys for the hydrogen evolution reaction, 4159
Metikoš-Huković, M., Omanović, S. and Jukić, A.
Impedance spectroscopy of semiconducting films on tin electrodes, 977
Meulenkamp, E.A., see Kelly, J.J., 561
Meyer, F., see Näfe, H., 1631
Michot, T., Nishimoto, A. and Watanabe, M.
Electrochemical properties of polymer gel electrolytes based on poly(vinylidene fluoride) copolymer and homopolymer, 1347
Mie, Y., Sonoda, K., Kishita, M., Krestyn, E., Neya, S., Funasaki, N. and Taniguchi, I.
Effect of rapid heme rotation on electrochemistry of myoglobin, 2903
Miecznikowski, K., see Malik, M.A., 3777
Min, M.-k., Cho, J., Cho, K. and Kim, H.
Particle size and alloying effects of Pt-based alloy catalysts for fuel cell applications, 4211
Misztal-Faraj, B., see Florjańczyk, Z., 3563
Mitsuishi, I., see Iwahori, T., 1509
Miwa, T., see Mehta, M.A., 1175
Miyawaki, T., see Taniguchi, I., 2843
Mizutani, F., see Hirata, Y., 2953
Mizutani, F., see Sato, Y., 2869
Mizutani, F., see Sawaguchi, T., 2861

Mizutani, F., Yabuki, S., Sato, Y., Sawaguchi, T. and Iijima, S.
Amperometric determination of pyruvate, phosphate and urea using enzyme electrodes based on pyruvate oxidase-containing poly(vinyl alcohol)/polyion complex-bilayer membrane, 2945
Modica, E., see Aricò, A.S., 4319
Molina, A., González, J., Saavedra, F. and Abrantes, L.M.
Cyclic reciprocal derivative chronopotentiometry. Applications to the detection and characterisation of adsorption processes, 761
Molina, A., see Abrantes, L.M., 457
Molnar, A., see Janik-Czachor, M., 3295
Momose, H., see Iwahori, T., 1509
Moncelli, M.R., see Krysinski, P., 1885
Monforte, G., see Aricò, A.S., 4319
Montilla, F., Huerta, F., Morallon, E. and Vazquez, J.L.
Electrochemical behaviour of benzene on platinum electrodes, 4271
Morales, E. and Acosta, J.L.
Synthesis and characterisation of poly(methylalkoxysiloxane) solid polymer electrolytes incorporating different lithium salts, 1049
Morales, G.M., see Barbero, C., 3895
Morallón, E., see Montilla, F., 4271
Morallón, E., see Quijada, C., 1847
Moreira, A.H., see Benedetti, A.V., 2187
Moressi, M.B., Zón, M.A. and Fernández, H.
Solvent effects on the heterogeneous kinetics of *N,N,N′,N′*-tetramethyl *p*-phenylendiamine (TMPD) in nonaqueous binary solvent mixtures. The role of the preferential solvation phenomenon, 1669
Mori, H., see Torimoto, T., 3269
Mori, K., see Fujinami, T., 1181
Mori, S., see Wang, X., 2677
Morimoto, T., Suzuki, K., Matsubara, T. and Yoshida, N.
Oxygen reduction electrode in brine electrolysis, 4257
Morin, S., see Allongue, P., 4591
Morino, S., see Yoshihara, S., 3375
Morita, J., see Kawahara, M., 1395
Morita, M., Araki, F., Kashiwamura, K., Yoshimoto, N. and Ishikawa, M.
Ionic structure and conductance behavior of plasticized polymeric electrolytes containing multivalent cations, 1335
Morita, M., see Yamada, O., 2197
Morlans, J.M., see Brillas, E., 4049
Mousty, C., Fóti, G., Comninellis, C. and Reid, V.
Electrochemical behaviour of DSA type electrodes prepared by induction heating, 451
Mullenix, A.N., see Kertesz, V., 1095
Münchow, V., Di Noto, V. and Tondello, E.
Poly[(oligoethylene glycol) dihydroxytitanate] as organic–inorganic polymer-electrolytes, 1211
Muñiz Alvarez, J.L., García Calzón, J.A. and López Fonseca, J.M.
Catalytic reduction of metal ions by adsorbed ligands in differential pulse voltammetry: evaluation of catalytic effects from the non-catalysed reduction peaks, 477
Murakami, S., see Ikeda, Y., 1167
Murakami, Y., see Takasu, Y., 4135
Muramatsu, N., see Tasaka, A., 3993
Murata, K., Izuchi, S. and Yoshihisa, Y.
An overview of the research and development of solid polymer electrolyte batteries, 1501
Muresan, L., see Dicu, D., 3951
Musiani, M.
Electrodeposition of composites: an expanding subject in electrochemical materials science, 3397
Musiani, M., see Cattarin, S., 2279
Muskal, N. and Mandler, D.
Thiol self-assembled monolayers on mercury surfaces: the adsorption and electrochemistry of ω-mercaptoalkanoic acids, 537
Mustarelli, P., see Capiglia, C., 1341
Myung, N., Kim, S., Lincot, D., Lepiller, C., de Tacconi, N.R. and Rajeshwar, K.
The deposition of Group 6A-derived inorganic semiconductor films as studied by quartz crystal microgravimetry, 3749

N

Näfe, H., Meyer, F. and Aldinger, F.
The equilibrium between Na-β- and Na-β″-alumina as a function of the phase composition, 1631
Nagasaki, Y., see Tsuruhara, K., 1391
Nagata, M., see Kawai, H., 315
Naji, A., Ghanbaja, J., Willmann, P. and Billaud, D.
New halogenated additives to propylene carbonate-based electrolytes for lithium-ion batteries, 1893
Nakagawa, Y., see Tasaka, A., 3993
Nakagima, T., see Gao, X.-P., 3099
Nakajima, N., see Iwahori, T., 1509
Nakajima, T., Koh, M., Gupta, V., Žemva, B. and Lutar, K.
Electrochemical behavior of graphite highly fluorinated by high oxidation state complex fluorides and elemental fluorine, 1655
Nakamatsu, S., see Yoshida, Y., 409
Nakamura, H., see Torimoto, T., 3269
Nakamura, H., see Yoshio, M., 273
Nakamura, N., see Okochi, M., 2917
Nakato, Y., see Zhou, X., 4655
Nakura, K., see Ohzuku, T., 151

Naohara, H., Ye, S. and Uosaki, K.
Electrocatalytic reactivity for oxygen reduction at epitaxially grown Pd thin layers of various thickness on Au(111) and Au(100), 3305
Naoi, K., see Suematsu, S., 3813
Naoi, K., Takeda, M., Kanno, H., Sakakura, M. and Shimada, A.
Simultaneous electrochemical formation of Al_2O_3/polypyrrole layers (I): effect of electrolyte anion in formation process, 3413
Natali, S., see Bozzini, B., 3431
Navarrete-Encina, P.A., see Núñez-Vergara, L.J., 3555
Navarro-Laboulais, J., see Sanmatías, A., 797
Navarro-Laboulais, J., see Trijueque, J., 789
Nazmutdinov, R.R., Tsirlina, G.A., Petrii, O.A., Kharkats, Y.I. and Kuznetsov, A.M.
Quantum chemical modelling of the heterogeneous electron transfer: from qualitative analysis to a polarization curve, 3521
Neumann, R., see Dobrev, D., 3117
Neya, S., see Mie, Y., 2903
Nguyen-Cong, H., see Ríos, E., 4431
Niaura, G.
Surface-enhanced Raman spectroscopic observation of two kinds of adsorbed OH^- ions at copper electrode, 3507
Nichols, R.J., see Raisch, P., 4635
Nie, L., see Zhou, A., 3943
Nikitin, E.V. and Zagumennov, V.A.
Initiation of homolytic addition to alkenes by means of organophosphorus radical-cations, 3983
Nikolenko, N.V., see Amadelli, R., 713
Nishiguchi, I., Itoh, K. and Maekawa, H.
Electrochemical hydrocoupling of acetylene derivatives by anodic oxidation of $NaBH_4$, 2991
Nishimoto, A., see Michot, T., 1347
Nishimoto, A., see Watanabe, M., 1187
Nishina, N., see Ito, K., 1295
Nishiura, M., see Kono, M., 1307
Nishiyama, K., see Li, C.-z., 2883
Nishizawa, M., see Kim, H.-S., 483
Niwa, D., see Takano, N., 3263
Noda, A. and Watanabe, M.
Highly conductive polymer electrolytes prepared by in situ polymerization of vinyl monomers in room temperature molten salts, 1265
Nohira, T., see Ito, Y., 2611
Novák, P., Imhof, R. and Haas, O.
Magnesium insertion electrodes for rechargeable nonaqueous batteries — a competitive alternative to lithium?, 351
Novák, P., see Joho, F., 3589
Núñez-Vergara, L.J., Squella, J.A., Olea-Azar, C., Bollo, S., Navarrete-Encina, P.A. and Sturm, J.C.
Nitrosobenzene: electrochemical, UV-visible and EPR spectroscopic studies on the nitrosobenzene free radical generation and its interaction with glutathione, 3555

O

Obata, R., see Goto, T., 3367
Oda, G., see Fuse, T., 2933
Oekermann, T., see Schlettwein, D., 4697
Oesten, R., see Levi, M.D., 1781
Ogata, N., see Kawahara, M., 1395
Ogata, N., see Tsuruhara, K., 1223
Ogata, N., see Tsuruhara, K., 1391
Ogata, S., see Yoshida, Y., 409
Ogata, Y.H., Ikeda, T., Sakka, T. and Kobayashi, T.
Influence of dissolved oxygen on intensity modulated photocurrent spectroscopy (IMPS) at a silicon–hydrofluoric acid interface, 2219
Ogumi, Z., see Funabiki, A., 865
Ogumi, Z., see Inaba, M., 99
Ogumi, Z., see Maruyama, J., 415
Oguro, K., see Asaka, K., 4517
Oh, S.M., see Kim, C.S., 2101
Ohashi, T., see Tasaka, A., 3993
Ohno, H., see Furukawa, T., 1443
Ohno, H., see Hirao, M., 1291
Ohno, H., see Ito, K., 1295
Ohno, H., see Kurusu, F., 2911
Ohno, H., see Tominaga, Y., 1285
Ohno, H., see Tominaga, Y., 3081
Ohno, H., see Yoshizawa, M., 1617
Ohsaka, T., see Fei Wu, J., 987
Ohsaka, T., see John, S.A., 1127
Ohsaka, T., see John, S.A., 4041
Ohsedo, Y., Imae, I. and Shirota, Y.
Electrochromic properties of new methacrylate copolymers containing pendant oligothiophene and oligo(ethyleneoxide) moieties in the presence of a polymer–gel electrolyte, 1543
Ohshita, J., see Tang, H., 2771
Ohshita, J., see Zhu, L., 2203
Ohtomo, M., see Arai, K., 3029
Ohtsuka, H., see Okada, S., 329
Ohzeki, K., see Abe, T., 4009
Ohzuku, T., Nakura, K. and Aoki, T.
Comparative study of solid-state redox reactions of $LiCo_{1/4}Ni_{3/4}O_2$ and $LiAl_{1/4}Ni_{3/4}O_2$ for lithium-ion batteries, 151
Okabe, T.H., see Jacob, K.T., 1963
Okada, S., Yamaki, J.-i., Asakura, K., Ohtsuka, H., Arai, H., Tobishima, S.-i. and Sakurai, Y.
Cathode characteristics of layered rocksalt oxide, Li_2PtO_3, 329
Okada, T., Yoshida, M., Hirose, T., Kasuga, K., Yu, T., Yuasa, M. and Sekine, I.
Oxygen reduction characteristics of graphite elec-

trodes modified with cobalt di-quinolyldiamine derivatives, 4419
Okajima, T., see Fei Wu, J., 987
Okochi, M., Nakamura, N. and Matsunaga, T.
Electrochemical killing of *Vibrio alginolyticus* using ferrocene-modified electrode, 2917
Olea-Azar, C., see Núñez-Vergara, L.J., 3555
Oliver, R., see Brillas, E., 4049
Omanović, S., see Metikoš-Huković, M., 977
O'Mullane, A.P., see Burke, L.D., 4127
Ono, T., see Iwahori, T., 1509
Onomura, O., see Matsumura, Y., 3011
Orel, B., see Švegl, F., 4359
Oropeza-Guzmán, M.T., see Cisneros-González, I., 2729
Osaka, T.
Electrodeposition of highly functional thin films for magnetic recording devices of the next century, 3311
Osaka, T., see Takano, N., 3263
Ossowski, T., Pipka, P., Liwo, A. and Jeziorek, D.
Electrochemical and UV-spectrophotometric study of oxygen and superoxide anion radical interaction with anthraquinone derivatives and their radical anions, 3581
Otero, M., see Barbero, C., 3895
Oura, Y., see Suematsu, S., 3813
Owens, B.B., Passerini, S. and Smyrl, W.H.
Lithium ion insertion in porous metal oxides, 215
Ozaki, Y., see Iwahori, T., 1509
Ozanam, F., see Chazalviel, J.-N., 3205
Ozil, P., see Antoine, O., 4493

P

Page, D., see Johannsen, K., 3691
Pagitsas, M., see Sazou, D., 2753
Paik, W., Yeo, I.-H., Suh, H., Kim, Y. and Song, E.
Ion transport in conducting polymers doped with electroactive anions examined by EQCM, 3833
Paillous, N., see Serpentini, C.-L., 1663
Pandey, J.P., see Singh, R.N., 1911
Panero, S., see Ericson, H., 1409
Pantano, E., see Decker, F., 4607
Papadopoulos, N., see Vetterl, V., 2961
Parilla, P.A., see McGraw, J.M., 187
Park, B.-K., see Gu, H.-B., 1533
Park, G.-C., see Gu, H.-B., 1533
Park, J.-K., see Kim, H.-T., 4001
Park, J.-K., see Lee, K.-H., 1301
Parkhutik, V.
New effects in the kinetics of the electrochemical oxidation of silicon, 3249
Parkinson, B.A., see Takeda, N., 4559
Passerini, S., see Appetecchi, G.B., 2139
Passerini, S., see Owens, B.B., 215
Pastor, E., see Rodríguez, J.L., 4279
Pastor, E., see Souto, R.M., 1645
Pastor, G., see Souto, R.M., 1645
Pauporté, T. and Lincot, D.
Electrodeposition of semiconductors for optoelectronic devices: results on zinc oxide, 3345
Pauporté, T., Andolfatto, F. and Durand, R.
Some electrocatalytic properties of anodic iridium oxide nanoparticles in acidic solution, 431
Pei, J., Li, X.-y. and Buffle, J.
Preparation, characterization and application of an electrode modified with electropolymerized $CuPtBr_6$ film, 1581
Peled, E., see Golodnitsky, D., 335
Peled, E., see Golodnitsky, D., 1431
Peled, E., see Strauss, E., 1519
Pereira, E.C., see Terezo, A.J., 4351
Pereira-Ramos, J.P., see Bach, S., 931
Perera, K., Dissanayake, M.A.K.L. and Bandaranayake, P.W.S.K.
Copper-ion conducting solid-polymer electrolytes based on polyacrylonitrile (PAN), 1361
Perkins, J.D., see McGraw, J.M., 187
Perrone, D., see Ratnakumar, B.V., 1513
Perrot, H., see García-Jareño, J.J., 3765
Persi, L., see Appetecchi, G.B., 23
Persi, L., see Appetecchi, G.B., 1481
Peter, L.M. and Wijayantha, K.G.U.
Electron transport and back reaction in dye sensitised nanocrystalline photovoltaic cells, 4543
Peter, L.M., Ponomarev, E.A., Franco, G. and Shaw, N.J.
Aspects of the photoelectrochemistry of nanocrystalline systems, 549
Peter, L.M., see Duffy, N.W., 3355
Petit, M.A., Plichon, V. and Colin, C.
A CV/PBD coupled study of ionic exchanges at poly(pyrrole) films in phosphate buffered solutions, 1953
Petrii, O.A., Safonova, T.Y., Tsirlina, G.A. and Rusanova, M.Y.
Nanoheterogeneous electrocatalysts fabricated by palladizing of platinum, 4117
Petrii, O.A., see Nazmutdinov, R.R., 3521
Pettinger, B., see Hoon-Khosla, M., 611
Pezzatini, G., see Forni, F., 3225
Piffard, Y., see Potiron, E., 197
Pineri, M., see Inzelt, G., 2403
Pinson, J., see Allongue, P., 3241
Pipka, P., see Ossowski, T., 3581
Plichon, V., see Petit, M.A., 1953
Poillerat, G., see González, M., 741
Poinsignon, C., see Depre, L., 1377
Poks, P., see Grzeszczuk, M., 4171
Ponomarev, E.A., see Peter, L.M., 549

Popall, M., see Depre, L., 1377
Popescu, I.C., see Dicu, D., 3951
Potiron, E., Le Gal La Salle, A., Verbaere, A., Piffard, Y. and Guyomard, D.
Electrochemically synthesized vanadium oxides as lithium insertion hosts, 197
Pouillerie, C., see Delmas, C., 243
Powell, S.M., see Böhm, S., 2165
Poznyak, S.K. and Kulak, A.I.
Characterization and photoelectrochemical properties of nanocrystalline In_2O_3 film electrodes, 1595
Prabhakara Rao, G., see Vittal, R., 2083
Prado, G., see Delmas, C., 243
Prakash, J. and Joachin, H.
Electrocatalytic activity of ruthenium for oxygen reduction in alkaline solution, 2289
Price, W.S., see Hayamizu, K., 1313
Prieto, F., see Barrado, E., 1105
Protsailo, L.V. and Fawcett, W.R.
Studies of electron transfer through self-assembled monolayers using impedance spectroscopy, 3497
Pshenichnikov, A.G., Burkal'tseva, L.A. and Kudryavtseva, Z.I.
Investigation of smooth and modified nickel surface by optoelectrochemical method, 4143
Pugh, D., see Berlouis, L.E.A., 623
Pyun, S.-I., see Han, J.-N., 2781
Pyun, S.-I., see Lee, W.-J., 1901
Pyun, S.-I., see Shin, H.-C., 489

Q

Qian, J., see Kjelstrup, S., 2707
Qian, R., see Li, Y., 1727
Qingfeng, L., Hjuler, H.A. and Bjerrum, N.J.
Oxygen reduction on carbon supported platinum catalysts in high temperature polymer electrolytes, 4219
Quijada, C., Huerta, F.J., Morallón, E., Vázquez, J.L. and Berlouis, L.E.A.
Electrochemical behaviour of aqueous SO_2 at polycrystalline gold electrodes in acidic media: a voltammetric and in situ vibrational study: Part 1. Reduction of SO_2: deposition of monomeric and polymeric sulphur, 1847
Quiroz, M.A., Córdova, F., Lamy-Pitara, E. and Barbier, J.
Electrocatalytic hydrogenation of *m*-xylene on platinized-platinum electrodes, 4291

R

Raisch, P., Haiss, W., Nichols, R.J. and Schiffrin, D.J.
In-situ atomic force microscopy of silicon(100) in aqueous potassium hydroxide, 4635
Rajalakshmi, N., Dhathathreyan, K.S., Govindaraj, A. and Satishkumar, B.C.
Electrochemical investigation of single-walled carbon nanotubes for hydrogen storage, 4511
Rajeshwar, K., see de Tacconi, N.R., 3403
Rajeshwar, K., see Myung, N., 3749
Ramakrishna, S., see Willig, F., 4565
Randler, R., see Giesen, M., 527
Rao, T.N., see Fujishima, A., 4683
Rappich, J., Timoshenko, V.Y., Würz, R. and Dittrich, T.
Is there a limit for the passivation of Si surfaces during anodic oxidation in acidic NH_4F solutions?, 4629
Ratnakumar, B.V., Smart, M.C., Huang, C.K., Perrone, D., Surampudi, S. and Greenbaum, S.G.
Lithium ion batteries for Mars exploration missions, 1513
Rauscher, S., see Lewerenz, H.J., 4615
Razzini, G., see Decker, F., 4607
Readey, D.W., see McGraw, J.M., 187
Rebrova, T.P., see Cherginets, V.L., 469
Reeve, R.W., Christensen, P.A., Dickinson, A.J., Hamnett, A. and Scott, K.
Methanol-tolerant oxygen reduction catalysts based on transition metal sulfides and their application to the study of methanol permeation, 4237
Reibel, L., see Alloin, F., 1193
Reiche, A., Weinkauf, A., Sandner, B., Rittig, F. and Fleischer, G.
Alternating copolymers for novel polymer electrolytes: the electrochemical properties, 1327
Reid, V., see Mousty, C., 451
Reineke-Koch, R., see Siemoneit, K., 4577
Reitzle, A., see Ziegler, J.C., 4599
Rethinaraj, J.P., see Kulandaisamy, S., 3047
Reymond, F., Fermín, D., Lee, H.J. and Girault, H.H.
Electrochemistry at liquid/liquid interfaces: methodology and potential applications, 2647
Rhoten, M.C., Burgess, J.D. and Hawkridge, F.M.
Temperature and pH effects on cytochrome *c* oxidase immobilized in an electrode-supported lipid bilayer membrane, 2855
Ricart, J.M., see Curulla, D., 639
Rikukawa, M., see Kawahara, M., 1395
Rikukawa, M., see Tsuruhara, K., 1391
Rikukawa, M., see Tsuruhara, K., 1223
Riley, D.J., see Hickey, S.G., 3277
Ristic, N.M., Kotorcevic, M., Lacnjevac, C.M., Jokic, A.M. and Jakšić, M.M.
Some specific potentiodynamic behaviour of certain aldehydes and monosaccharides: Some simple and some specific aldehydes, 2973
Ristovski, G., see Belca, I.D., 4059
Ristovski, L., see Belca, I.D., 4059
Ritala, M., see Kemell, M., 3737

Rittig, F., see Reiche, A., 1327
Robertson, A.D., see Armstrong, A.R., 285
Roca, I., see Martínez-Ortiz, F., 387
Rodríguez, J.L. and Pastor, E.
A comparative study on the adsorption of benzyl alcohol, toluene and benzene on platinum, 4279
Rodríguez, J.L., see Souto, R.M., 1645
Rogers, K.D., see Duffy, N.W., 3355
Rogers, K.R., Becker, J.Y. and Cembrano, J.
Improved selective electrocatalytic oxidation of phenols by tyrosinase-based carbon paste electrode biosensor, 4373
Rojas-Chapana, J.A., see Tributsch, H., 4705
Romagnoli, P., see Appetecchi, G.B., 23
Romagnoli, R., see Borrás, C.A., 1717
Ronci, F., see Appetecchi, G.B., 1481
Ríos, E., Nguyen-Cong, H., Marco, J.F., Gancedo, J.R., Chartier, P. and Gautier, J.L.
Indirect oxidation of ethylene glycol by peroxide ions at $Ni_{0.3}Co_{2.7}O_4$ spinel oxide thin film electrodes, 4431
Rosenmund, J., see Eickes, C., 3623
Ross, P.N., see Marković, N.M., 4101
Rougier, A., see Delmas, C., 243
Roy, S., see Johannsen, K., 3691
Rubinson, J.F., see Mark, H.B., Jr., 4309
Rudd, A.L. and Breslin, C.B.
Photo-induced dissolution of zinc in alkaline solutions, 1571
Rudd, A.L. and Breslin, C.B.
The electrochemical behaviour of CuZn under conditions of illumination, 4015
Rüetschi, P., see Beck, F., 2467
Rusanova, M.Y., see Petrii, O.A., 4117
Rusling, J.F., see Carrero, H., 503
Rzeznik, M., see Gu, G.Y., 3127

S

Saadoune, I., see Delmas, C., 243
Saario, T., see Bojinov, M., 2029
Saario, T., see Bojinov, M., 2791
Saavedra, F., see Abrantes, L.M., 457
Saavedra, F., see Molina, A., 761
Sablé, E., see Simon, E., 855
Sada, T., see Kono, M., 1307
Sa Ferreira, R.A., see Carlos, L.D., 1555
Safi, M., see Chazalviel, J.-N., 3205
Safonov, V.A., see Sottomayor, M.J., 775
Safonova, T.Y., see Petrii, O.A., 4117
Saidman, S.B. and Bessone, J.B.
The influence of electrode material on NAD^+ oxidation, 3151
Saito, M., Endo, A., Shimizu, K. and Satô, G.P.
Electrochemical polymerization of tetraphenylporphyrinatoruthenium(II) complexes with diaza compounds as axial ligands, 3021
Saito, Y., see Capiglia, C., 1341
Sakakura, M., see Naoi, K., 3413
Sakata, T., see Torimoto, T., 3269
Sakka, T., see Ogata, Y.H., 2219
Sakmeche, N., Aaron, J.-J., Aeiyach, S. and Lacaze, P.-C.
Usefulness of aqueous anionic micellar media for electrodeposition of poly-(3,4-ethylenedioxythiophene) films on iron, mild steel and aluminium, 1921
Sakurai, M., see Tanaka, R., 1385
Sakurai, Y., see Okada, S., 329
Saleh, M.M.
Mathematical modeling of gas evolving flow-through porous electrodes, 959
Salmon, E., see Vassal, N., 1527
Saloniemi, H., see Kemell, M., 3737
Samec, Z., Lhotský, A. and Mareček, V.
Peculiar correlation between the interfacial capacity and faradaic admittance of the ion transfer across an interface between two immiscible electrolyte solutions, 583
Sánchez, C. and Leiva, E.P.M.
Cu underpotential deposition on Au(111) and Au(100). Can this be explained in terms of the energetics of the Cu/Au system?, 691
Sanchez, J.-Y., see Alloin, F., 1193
Sanchez, J.-Y., see Saunier, J., 1255
Sanchez, L., see Bach, S., 931
Sánchez, M.D., see Calvente, J.J., 3087
Sandhu, S.S. and Fellner, J.P.
Thermodynamic equations for a model lithium-ion cell, 969
Sandner, B., see Reiche, A., 1327
Sanmatías, A., Benito, D., Navarro-Laboulais, J., García-Jareño, J.J. and Vicente, F.
Surface modification of graphite + polymer composite and ITO electrodes by Nafion® + cupromeronic phthalocyanine films, 797
Sanmatías, A., see García-Jareño, J.J., 3765
Sanmatías, A., see Trijueque, J., 789
Sanui, K., see Kawahara, M., 1395
Sanui, K., see Tsuruhara, K., 1391
Sanui, K., see Tsuruhara, K., 1223
Satishkumar, B.C., see Rajalakshmi, N., 4511
Satô, G.P., see Saito, M., 3021
Sato, T., see Arai, K., 3029
Sato, Y. and Mizutani, F.
Electrochemical responses of cytochrome *c* on gold electrodes modified with nucleic acid base derivatives–electrochemical and quartz crystal microbalance studies, 2869

Sato, Y., see Mizutani, F., 2945
Satoh, Y., see Matsumura, Y., 3011
Saunier, J., Alloin, F. and Sanchez, J.-Y.
Electrochemical and spectroscopic studies of polymethacrylonitrile based electrolytes, 1255
Savadogo, O., see Tazi, B., 4329
Savinell, R.F., see Gojković, S.L., 889
Savy, M., see Contamin, O., 721
Sawaguchi, T., Mizutani, F., Yoshimoto, S. and Taniguchi, I.
Voltammetric and in situ STM studies on self-assembled monolayers of 4-mercaptopyridine, 2-mercaptopyridine and thiophenol on Au(111) electrodes, 2861
Sawaguchi, T., see Mizutani, F., 2945
Sazou, D., Diamantopoulou, A. and Pagitsas, M.
Chemical perturbation of the passive–active transition state of Fe in a sulfuric acid solution by adding halide ions. Current oscillations and stability of the iron oxide film, 2753
Scarbeck, G., see Contamin, O., 721
Schell, M., see Chen, S., 3069
Scherson, D.A., see Totir, D.A., 161
Schiffrin, D.J., see Raisch, P., 4635
Schlettwein, D., Karmann, E., Oekermann, T. and Yanagi, H.
Wavelength-dependent switching of the photocurrent direction at the surface of molecular semiconductor electrodes based on orbital-confined excitation and transfer of charge carriers from higher excited states, 4697
Schmickler, W., see Guidelli, R., 2317
Schmidt, U., see Schwanbeck, H., 4389
Schmidt, W., see Grundmeier, G., 2515
Schmieder, H., see Jüttner, K., 2575
Schmitz, C., see Krumm, R., 3255
Schmutz, P. and Landolt, D.
Electrochemical quartz crystal microbalance study of the transient response of passive Fe–25Cr alloy, 899
Schneeweiss, M.A., see Hagenström, H., 1141
Schultze, J.W.
Electrochemical Materials Science: An introduction to Symposium 4 of the 50th Anniversary of ISE 'Electrochemistry and Materials: Synthesis and Characterization', 3193
Schultze, J.W. and Lohrengel, M.M.
Stability, reactivity and breakdown of passive films. Problems of recent and future research, 2499
Schultze, J.W., see Inzelt, G., 2403
Schwanbeck, H. and Schmidt, U.
Preparation and characterisation of magnetic nanostructures using filtration membranes, 4389
Schwitzgebel, G., see Bund, A., 3703
Scott, K., Taama, W.M., Kramer, S., Argyropoulos, P. and Sundmacher, K.
Limiting current behaviour of the direct methanol fuel cell, 945
Scott, K., see Argyropoulos, P., 1983
Scott, K., see Reeve, R.W., 4237
Scrosati, B.
Recent advances in lithium ion battery materials, 2461
Scrosati, B., see Appetecchi, G.B., 23
Scrosati, B., see Appetecchi, G.B., 1481
Scrosati, B., see Ericson, H., 1409
Seeber, R., see Giorgetti, M., 4475
Sekiguchi, R., see Ikezawa, Y., 1089
Sekine, I., see Okada, T., 4419
Senboku, H., Fujimura, Y., Kamekawa, H. and Tokuda, M.
Divergent electrochemical carboxylation of vinyl triflates: new electrochemical synthesis of phenyl-substituted α,β-unsaturated carboxylic acids and aliphatic β-keto carboxylic acids, 2995
Senthil Kumar, A., see Zen, J.-M., 1691
Seo, M., see Hassel, A.W., 4673
Serpentini, C.-L., Gauchet, C., de Montauzon, D., Comtat, M., Ginestar, J. and Paillous, N.
First electrochemical investigation of the redox properties of DOPA–melanins by means of a carbon paste electrode, 1663
Shaban, A., see Telegdi, J., 3639
Shahnazaryan, G.E., see Aroutiounian, V.M., 1999
Shaw, N.J., see Peter, L.M., 549
Shi, Z., see Liu, T., 2743
Shibuya, M., see Ikezawa, Y., 2075
Shim, J., Yoo, D.-Y. and Lee, J.-S.
Characteristics for electrocatalytic properties and hydrogen–oxygen adsorption of platinum ternary alloy catalysts in polymer electrolyte fuel cell, 1943
Shimada, A., see Naoi, K., 3413
Shimamune, T., see Yoshida, Y., 409
Shimizu, K., Habazaki, H., Skeldon, P., Thompson, G.E. and Wood, G.C.
Migration of sulphate ions in anodic alumina, 1805
Shimizu, K., see Saito, M., 3021
Shin, H.-C. and Pyun, S.-I.
The kinetics of lithium transport through $Li_{1-\delta}$-CoO_2 by theoretical analysis of current transient, 489
Shin, H.K., see Choi, B.K., 1371
Shinozaki, K., see Yoshihara, S., 3375
Shiraga, S., see Iwahori, T., 1509
Shirakashi, T., see Yoshihara, S., 3375
Shirota, Y., see Ohsedo, Y., 1543
Shirota, Y., see Yasuda, Y., 1537
Shono, A., see Tanaka, R., 1385
Shouji, E. and Buttry, D.A.
EQCM measurements of solvent transport during Li^+ intercalation in V_2O_5 xerogel films, 3757

Shumsky, M.G., see Vertegel, A.A., 3233
Siemoneit, K., Reineke-Koch, R., Meier, A. and Memming, R.
Fast processes at semiconductor–liquid interfaces: reactions at GaAs electrodes, 4577
Sikora, E., see Sikora, J., 1875
Sikora, J., Sikora, E. and Macdonald, D.D.
The electronic structure of the passive film on tungsten, 1875
Sikorski, K., see Janik-Czachor, M., 3295
Silberg, I.A., see Dicu, D., 3951
Silva, F., see Sottomayor, M.J., 775
Silva, M.M. and Smith, M.J.
Preparation and characterization of a polymer electrolyte based on europium picrate, 1463
Silva, M.M., de Zea Bermudez, V., Carlos, L.D. and Smith, M.J.
Thermal properties and ionic conductivities of lanthanide-based ormolytes, 1467
Silva, R., see Dávila Jiménez, M.M., 4187
Simon, B., see Broussely, M., 3
Simon, B., see Guerin, K., 1607
Simon, E., Sablé, E., Handel, H. and L'Her, M.
Electrodes modified by conducting polymers bearing redox sites: Ni- and Co-cyclam complexes on polypyrrole, 855
Singh, N.K., see Singh, R.N., 1911
Singh, R.N., Pandey, J.P., Singh, N.K., Lal, B., Chartier, P. and Koenig, J.-F.
Sol-gel derived spinel $M_xCo_{3-x}O_4$ ($M = Ni$, Cu; $0 \leq x \leq 1$) films and oxygen evolution, 1911
Siow, K.S., see Dai, J., 2211
Skeldon, P., see Shimizu, K., 1805
Skompska, M.
Quartz crystal microbalance study of electrochemical deposition of poly(3-dodecylthiophene) films on Au electrodes, 3841
Smart, M.C., see Ratnakumar, B.V., 1513
Smith, K., see Vermeulen, L.A., 1007
Smith, M.J., see Silva, M.M., 1463
Smith, M.J., see Silva, M.M., 1467
Smyrl, W.H., see Owens, B.B., 215
Soavi, F., see Arbizzani, C., 2273
Södervall, U., see Mattsson, J., 1453
Song, E., see Paik, W., 3833
Song, H.-K., Hwang, H.-Y., Lee, K.-H. and Dao, L.H.
The effect of pore size distribution on the frequency dispersion of porous electrodes, 2241
Song, H.-W., see Gu, H.-B., 1533
Song, W., Liu, Y., Lu, N., Xu, H. and Sun, C.
Application of the sol-gel technique to polyoxometalates: towards a new chemically modified electrode, 1639
Sonoda, K., see Mie, Y., 2903
Sotiriou-Leventis, C., see Collins, C.M., 2049
Sottomayor, M.J., Coelho, V., Ferreira, A.P., Silva, F., Baturina, O.A., Safonov, V.A. and Damaskin, B.B.
Parameters of *n*-hexanol adsorption on Au (111). Comparison between differential capacity and chronocoulometry results, 775
Soula, B., see Fabre, P.-L., 2697
Souto, R.M., Rodríguez, J.L., Pastor, G. and Pastor, E.
Investigation of the electrochemical reactivity of benzyl alcohol at platinum and palladium electrodes, 1645
Spichiger, U.E., see Zhang, W., 2259
Spitler, M.T., see Ehret, A., 4553
Squella, J.A., see Núñez-Vergara, L.J., 3555
Stafiej, J., Borkowska, Z. and Badiali, J.P.
A simple description of ionic desorption observed in differential capacitance data, 3489
Staikov, G., see Budevski, E., 2559
Staikov, G., see Krumm, R., 3255
Stalnionis, G., see Jusys, Z., 3675
Stepanyan, G.M., see Aroutiounian, V.M., 1999
Stimming, U., see Friedrich, K.A., 3283
Stojek, Z., see Donten, M., 3389
Storck, W., see Willig, F., 4565
Strandberg, M., see Idla, K., 2121
Strašák, L., see Vetterl, V., 2961
Stratmann, M., see Grundmeier, G., 2515
Strauss, E., Golodnitsky, D. and Peled, E.
Study of phase changes during 500 full cycles of Li/composite polymer electrolyte/FeS_2 battery, 1519
Strehblow, H.-H., see Alonso-Vante, N., 4227
Stuhl, L., see Ehret, A., 4553
Sturm, J.C., see Núñez-Vergara, L.J., 3555
Stygar, J., Zalewska, A. and Wieczorek, W.
Studies of ionic interactions in low molecular weight polyether electrolytes, 1437
Subramanian, R. and Lakshminarayanan, V.
A study of kinetics of adsorption of alkanethiols on gold using electrochemical impedance spectroscopy, 4501
Subramanian, V.R., see Botte, G.G., 2595
Suda, S., see Gao, X.-P., 3099
Suda, S., see Li, Z.P., 1773
Suematsu, S., Oura, Y., Tsujimoto, H., Kanno, H. and Naoi, K.
Conducting polymer films of cross-linked structure and their QCM analysis, 3813
Sueoka, T., see Arai, K., 3029
Sugie, K., see Fujinami, T., 1181
Sugimoto, S., see Tasaka, A., 3993
Suh, H., see Paik, W., 3833
Sun, C., see Song, W., 1639
Sun, I.-W., see Chen, P.-Y., 441
Sun, I.-W., see Chen, P.-Y., 3163
Sun, J., see Ferry, A., 1237
Sun, J., see McFarlane, D.R., 1271
Sun, S.-G., see Wu, Q.-H., 3683
Sun, S.-G., see Xiao, X.-Y., 2897

Sun, Y.-M., see Gao, X.-P., 3099
Sunatsuki, Y., see Taniguchi, I., 2843
Sundholm, F., see Mattsson, B., 1405
Sundholm, G., see Bojinov, M., 2029
Sundholm, G., see Bojinov, M., 2791
Sundmacher, K., see Scott, K., 945
Surampudi, S., see Ratnakumar, B.V., 1513
Suzuki, K., see Morimoto, T., 4257
Suzuki, Y., see Watanabe, M., 1187
Svanberg, C., see Ericson, H., 1409
Švegl, F., Orel, B., Grabec-Švegl, I. and Kaučič, V.
Characterization of spinel Co_3O_4 and Li-doped Co_3O_4 thin film electrocatalysts prepared by the sol–gel route, 4359
Swenson, J., see Carlsson, P., 1449
Switzer, J.A., see Vertegel, A.A., 3233
Szummer, A., see Janik-Czachor, M., 3295

T

Taama, W.M., see Argyropoulos, P., 1983
Taama, W.M., see Scott, K., 945
Tadini-Buoninsegni, F., see Krysinski, P., 1885
Tadjeddine, A. and Le Rille, A.
Adsorption of cyanide on gold single crystal investigated by in situ visible–infrared difference frequency generation, 601
Tadjeddine, A., see Etgens, V.H., 591
Taira, H., see Taniguchi, I., 2843
Takahashi, Y., see Furukawa, T., 1443
Takamura, K., see Arai, K., 3029
Takamura, K., see Fuse, T., 2933
Takano, N., Niwa, D., Yamada, T. and Osaka, T.
Nickel deposition behavior on n-type silicon wafer for fabrication of minute nickel dots, 3263
Takasu, Y. and Murakami, Y.
Design of oxide electrodes with large surface area, 4135
Takeda, M., see Naoi, K., 3413
Takeda, N. and Parkinson, B.A.
The relationship between squaraine dye surface morphology and sensitization behavior on SnS_2 electrodes, 4559
Takeuchi, K., see Iwahori, T., 1509
Takizawa, N., see Tominaga, Y., 1285
Talbot, J.B., see Ahlers, C.B., 3379
Tamanouchi, H., see Arai, K., 3029
Tanaka, R., Yamamoto, H., Shono, A., Kubo, K. and Sakurai, M.
Proton conducting behavior in non-crosslinked and crosslinked polyethylenimine with excess phosphoric acid, 1385
Tang, H., see Zhu, L., 2203
Tang, H., Zhu, L., Harima, Y., Kunugi, Y., Yamashita, K., Ohshita, J. and Kunai, A.
Optical study on electrochemical and chemical doping of polymers of oligothienyls bridged by monosilyl, 2771
Tang, S.C., see Bouwkamp-Wijnoltz, A.L., 379
Taniguchi, I., see Li, C.-z., 2883
Taniguchi, I., see Mie, Y., 2903
Taniguchi, I., see Sawaguchi, T., 2861
Taniguchi, I., Yoshimoto, S., Yoshida, M., Kobayashi, S.-i., Miyawaki, T., Aono, Y., Sunatsuki, Y. and Taira, H.
Simple methods for preparation of a well-defined 4-pyridinethiol modified surface on Au(111) electrodes for cytochrome *c* electrochemistry, 2843
Taniguchi, S., see Iwahori, T., 1509
Tarascon, J.-M., see Amatucci, G., 255
Tasaka, A., Ohashi, T., Muramatsu, N., Nakagawa, Y. and Sugimoto, S.
Behavior of thermally oxidized and fluorinated nickel anodes in molten $NH_4F{\cdot}2HF$, 3993
Tavares, A.C. and Trasatti, S.
$Ni + RuO_2$ co-deposited electrodes for hydrogen evolution, 4195
Tazi, B. and Savadogo, O.
Parameters of PEM fuel-cells based on new membranes fabricated from Nafion®, silicotungstic acid and thiophene, 4329
Teeters, D., see Le Granvalet-Mancini, M., 1491
Tegenfeldt, J., see Johansson, P., 3055
Tegenfeldt, J., see Ludvigsson, M., 2267
Telegdi, J., Shaban, A. and Kálmán, E.
EQCM study of copper and iron corrosion inhibition in presence of organic inhibitors and biocides, 3639
Terashima, H., see Ikezawa, Y., 2075
Terezo, A.J. and Pereira, E.C.
Fractional factorial design applied to investigate properties of $Ti/IrO_2–Nb_2O_5$ electrodes, 4351
Teshima, K., see Kim, Y., 1549
Thevenot, L., see Billaud, D., 59
Thomas, J.O., see Aabloo, A., 1425
Thomas, P., Ghanbaja, J. and Billaud, D.
Electrochemical insertion of sodium in pitch-based carbon fibres in comparison with graphite in $NaClO_4$–ethylene carbonate electrolyte, 423
Thompson, G.E., see Shimizu, K., 1805
Tikhomirova, A.V., see Kondratiev, V.V., 751
Timoshenko, V.Y., see Rappich, J., 4629
Tirado, J.L., see Bach, S., 931
Tobishima, S.-i., see Okada, S., 329
Tokida, A., see Aoki, K., 3483
Tokuda, K., see Fei Wu, J., 987
Tokuda, K., see John, S.A., 4041
Tokuda, M., see Senboku, H., 2995
Tominaga, Y. and Ohno, H.
Lithium ion conduction in linear- and network-type polymers of PEO/sulfonamide salt hybrid, 3081

Tominaga, Y., Takizawa, N. and Ohno, H.
Effect of added salt species on the ionic conductivity of PEO/sulfonamide salt hybrids, 1285
Tondello, E., see Münchow, V., 1211
Tong, Y., see Liu, P., 2147
Torell, L.M., see Carlsson, P., 1449
Torell, L.M., see Mattsson, B., 1405
Torell, L.M., see Mattsson, J., 1453
Torimoto, T., Tsumura, N., Nakamura, H., Kuwabata, S., Sakata, T., Mori, H. and Yoneyama, H.
Photoelectrochemical properties of size-quantized semiconductor photoelectrodes prepared by two-dimensional cross-linking of monodisperse CdS nanoparticles, 3269
Totir, D.A., Cahan, B.D. and Scherson, D.A.
Electrochemical characterization of lithiated transition metal oxide cathode particles in the absence of carbon, binders and other additivies, 161
Touzain, S., see Deslouis, C., 1837
Toyoda, E., see Gao, X.-P., 3099
Trasatti, S.
Electrocatalysis: understanding the success of DSA®, 2377
Trasatti, S., see Tavares, A.C., 4195
Tribollet, B., see Deslouis, C., 1837
Tribollet, B., see Herbert-Guillou, D., 1067
Tributsch, H. and Rojas-Chapana, J.A.
Metal sulfide semiconductor electrochemical mechanisms induced by bacterial activity, 4705
Trijueque, J., García-Jareño, J.J., Navarro-Laboulais, J., Sanmatías, A. and Vicente, F.
Ohmic drop of Prussian-blue/graphite + epoxy electrodes, 789
Tryk, D.A., Fujishima, A. and Honda, K.
Recent topics in photoelectrochemistry: achievements and future prospects, 2363
Tryk, D.A., see Fujishima, A., 4683
Tryk, D.A., see Yoshihara, S., 3375
Tsionsky, V., see Daikhin, L., 3615
Tsionsky, V., see Zilberman, G., 3473
Tsirlina, G.A., see Nazmutdinov, R.R., 3521
Tsirlina, G.A., see Petrii, O.A., 4117
Tsujimoto, H., see Suematsu, S., 3813
Tsumura, N., see Torimoto, T., 3269
Tsuruhara, K., Hara, K., Kawahara, M., Rikukawa, M., Sanui, K. and Ogata, N.
Ion conductivity of poly(ethylene oxide)/ligand complexes with the hydrogen-bond interaction, 1223
Tsuruhara, K., Rikukawa, M., Sanui, K., Ogata, N., Nagasaki, Y. and Kato, M.
Synthesis of proton conducting polymer based on poly(silamine), 1391
Tsymbal, L.V., see de Alwis, C., 2061
Tukamoto, H., see Kawai, H., 315
Turner, J.A., see Aroutiounian, V.M., 1999
Tymosiak-Zielińlska, A. and Borkowska, Z.
Interfacial properties of polycrystalline gold electrode in tetramethylammonium hydroxide solutions, 3105

U

Uchida, I., see Kim, H.-S., 483
Uda, T., see Jacob, K.T., 1963
Ulstrup, J., see Kuznetsov, A.M., 2339
Ungar, G., see Zheng, Y., 1161
Unkauf, W., see Friedrich, K.A., 3283
Uosaki, K., see Naohara, H., 3305
Urbakh, M., see Daikhin, L., 3615
Urbakh, M., see Daikhin, L.I., 685

V

Väärtnõu, M. and Lust, E.
Calculation of the characteristics of Cl^- and Br^- ions adsorption on bismuth single-crystal planes from solutions in 2-propanol, 1623
Väärtnõu, M., see Lust, K., 3543
Van der Ven, A., see Ceder, G., 131
van der Wal, P.D., see Koudelka-Hep, M., 2437
Van krieken, M. and Buess-Herman, C.
On the adsorption of uridine at the Ag(111)/aqueous solution interface, 675
van Veen, J.A.R., see Bouwkamp-Wijnoltz, A.L., 379
Varga, M., see Janik-Czachor, M., 3295
Vargas, M.A., Vargas, R.A. and Mellander, B.-E.
More studies on the PVAl + H_3PO_2 + H_2O proton conductor gels, 1399
Vargas, R.A., see Vargas, M.A., 1399
Vasilic, R., see Belca, I., 993
Vassal, N., Salmon, E. and Fauvarque, J.-F.
Electrochemical properties of an alkaline solid polymer electrolyte based on P(ECH-co-EO), 1527
Vaughn, W., see Mark, H.B., Jr., 4309
Vázquez, J.L., see Montilla, F., 4271
Vázquez, J.L., see Quijada, C., 1847
Velichenko, A.B., Amadelli, R., Zucchini, G.L., Girenko, D.V. and Danilov, F.I.
Electrosynthesis and physicochemical properties of Fe-doped lead dioxide electrocatalysts, 4341
Velichenko, A.B., see Amadelli, R., 713
Venkateswaran, K.V., see Kulandaisamy, S., 3047
Verbaere, A., see Potiron, E., 197
Vermeulen, L.A., Smith, K. and Wang, J.
Electrochemical polymerization of alkyltrichlorosilane monomers to form branched Si backbone polymers, 1007
Vermoyal, J.J., Frichet, A., Dessemond, L. and Hammou, A.
AC impedance study of corrosion films formed on zirconium based alloys, 1039

Vertegel, A.A., Shumsky, M.G. and Switzer, J.A.
Epitaxial electrodeposition of thallic oxide on single crystal gold, 3233
Vetter, J., see Dobrev, D., 3117
Vetterl, V., Papadopoulos, N., Dražan, V., Strašák, L., Hasoň, S. and Dvořák, J.
Nucleic acid sensing by impedance measurements, 2961
Vicente, F., see García-Jareño, J.J., 3765
Vicente, F., see Sanmatías, A., 797
Vicente, F., see Trijueque, J., 789
Vieil, E., see Henderson, M.J., 3885
Vilar, J., see Brillas, E., 4049
Visscher, W., see Bouwkamp-Wijnoltz, A.L., 379
Visvanathan, S., see Kulandaisamy, S., 3047
Visy, C. and Kankare, J.
Direct in situ conductance evidence for non-faradaic electrical processes in poly(3-methylthiophene), 1811
Visy, C., Kankare, J. and Kriván, E.
EQCM and in situ conductance studies on the polymerisation and redox features of thiophene copolymers, 3851
Vitins, G., see West, K., 3141
Vittal, R., Gomathi, H. and Prabhakara Rao, G.
Influence of a cationic surfactant on the modification of electrodes with nickel hexacyanoferrate surface films, 2083
Vogt, H., see Eigeldinger, J., 4449
Vojnović, M.V., see Jakšić, J.M., 4151
Vondrák, J., see Bezdička, P., 913
Vorotyntsev, M.A., see Inzelt, G., 2403

W

Wada, Y., see Ikeda, Y., 1167
Wandlowski, T., see Dretschkow, T., 731
Wang, B., see Liu, S., 1683
Wang, J., see Vermeulen, L.A., 1007
Wang, J.X., see Adžić, R.R., 4203
Wang, K., see Eickes, C., 3623
Wang, R.L., see Duffy, N.W., 3355
Wang, X., Yasukawa, E. and Mori, S.
Inhibition of anodic corrosion of aluminum cathode current collector on recharging in lithium imide electrolytes, 2677
Wark, A.W., see Berlouis, L.E.A., 623
Waseda, Y., see Jacob, K.T., 1963
Wasle, S., see Eickes, C., 3623
Watanabe, M., see Michot, T., 1347
Watanabe, M., see Noda, A., 1265
Watanabe, M., Suzuki, Y. and Nishimoto, A.
Single ion conduction in polyether electrolytes alloyed with lithium salt of a perfluorinated polyimide, 1187
Wayner, D.D.M., see Allongue, P., 4591
Wei, M., Li, N., Gu, Z. and Zhou, X.
Electrochemical behavior of films of C_{60}-dimethyl-(β-cyclodextrin) (1:1 and 1:2) inclusion complexes in mixed water and acetonitrile solutions, 4441
Wei, R.P., see Liao, C.-M., 881
Weil, K.G., see Eickes, C., 3623
Weinkauf, A., see Reiche, A., 1327
Weissman, I., see Aurbach, D., 67
Weissman, I., see Aurbach, D., 1135
Wendt, H., see Janowitz, K., 1025
Wennerberg, A., see Mattsson, J., 1453
West, A.R., see Kawai, H., 315
West, K., Vitins, G. and Koksbang, R.
Synthesis and host properties of tetragonal $Li_2Mn_2O_4$ and $Li_2Co_{0.4}Mn_{1.6}O_4$, 3141
White, R.E., see Botte, G.G., 2595
Wieczorek, W., see Stygar, J., 1437
Wielgosz, R.I., see Ziegler, J.C., 827
Wijayantha, K.G.U., see Peter, L.M., 4543
Wilde, C.P., De Cliff, S.V., Hui, K.C.A. and Brett, D.J.L.
The influence of adsorbed hydrogen and extended cycling on the EQCM response of electrodeposited Pt electrodes, 3649
Wilde, C.P., see Kucernak, A.R., 4483
Williams, D.E., see Kucernak, A.R., 4483
Willig, F., Zimmermann, C., Ramakrishna, S. and Storck, W.
Ultrafast dynamics of light-induced electron injection from a molecular donor into the wide conduction band of a semiconductor as acceptor, 4565
Willmann, P., see Billaud, D., 59
Willmann, P., see Geoffroy, I., 2019
Willmann, P., see Naji, A., 1893
Wilmott, M., see Cheng, Y.F., 1763
Wilson, G.S., see Armstrong, F.A., 2623
Winter, M. and Besenhard, J.O.
Electrochemical lithiation of tin and tin-based intermetallics and composites, 31
Wood, G.C., see Shimizu, K., 1805
Worsley, D.A., see Böhm, S., 2165
Wright, P.V., see Zheng, Y., 1161
Wu, C., see Gu, G.Y., 3127
Wu, H., see Gong, J., 1753
Wu, K., see Zei, M.S., 809
Wu, L.L., Huang, H.G., Li, J.X., Luo, J. and Lin, Z.H.
Time-resolved UV-vis spectroelectrochemical studies of the electron transfer process of cytochrome *c*, 2877
Wu, L., Zhou, J., Luo, J. and Lin, Z.
Oxidation and adsorption of deoxyribonucleic acid at highly ordered pyrolytic graphite electrode, 2923
Wu, Q.-H., Sun, S.-G., Xiao, X.-Y., Yang, Y.-Y. and Zhou, Z.-Y.
An EQCM study of Sb adsorption and coadsorp-

tion with CO on Pt electrode in perchloric acid solutions, 3683
Würz, R., see Rappich, J., 4629

X

Xia, S.J. and Birss, V.I.
In situ mass and ellipsometric study of hydrous oxide film growth on Pt in alkaline solutions, 3659
Xia, X.H. and Kelly, J.J.
The influence of oxidizing agents on etching and passivation of silicon in KOH solution, 4645
Xia, X.H.
New insights into the influence of upd Sn on the oxidation of formic acid on platinum in acidic solution, 1057
Xia, Y., see Yoshio, M., 273
Xiao, X.-Y. and Sun, S.-G.
Electrosorption of *p*-nitrobenzoic acid at a gold electrode in perchloric acid solutions studied by using cyclic voltammetry, EQCM, in situ FTIRS and Raman spectroscopy, 2897
Xiao, X.-Y., see Wu, Q.-H., 3683
Xie, N., see Zhou, A., 3943
Xie, Q., see Zhou, A., 3943
Xu, H., see Song, W., 1639
Xu, K., see Zhang, S., 1229

Y

Yabuki, S., see Mizutani, F., 2945
Yamada, O., Ishikawa, M. and Morita, M.
Charge/discharge cycling and impedance response of $LiMn_2O_4$ electrode in organic electrolyte solutions with different compositions, 2197
Yamada, T., see Takano, N., 3263
Yamaki, J.-i., see Okada, S., 329
Yamamoto, H., see Capiglia, C., 1341
Yamamoto, H., see Tanaka, R., 1385
Yamamoto, O.
Solid oxide fuel cells: fundamental aspects and prospects, 2423
Yamashita, K., see Tang, H., 2771
Yamashita, K., see Zhu, L., 2203
Yan, C.W., Lin, H.C. and Cao, C.N.
Investigation of inhibition of 2-mercaptobenzoxazole for copper corrosion, 2815
Yanagi, H., see Schlettwein, D., 4697
Yang, Q. and Luo, J.L.
The hydrogen-enhanced effects of chloride ions on the passivity of type 304 stainless steel, 3927
Yang, Q., see Liu, P., 2147
Yang, Y., see Liu, P., 2147
Yang, Y.-Y., see Wu, Q.-H., 3683
Yao, S., see Zhou, A., 3943
Yasuda, Y., Kamiyama, T. and Shirota, Y.
Ionic conductivities of low molecular-weight organic gels and their application as electrochromic materials, 1537
Yasukawa, E., see Wang, X., 2677
Yazami, R.
Surface chemistry and lithium storage capability of the graphite–lithium electrode, 87
Ye, S., see Naohara, H., 3305
Yeo, I.-H., see Kim, S.H., 2889
Yeo, I.-H., see Paik, W., 3833
Yokoyama, H., see Hirata, Y., 2953
Yoneya, K., see Furukawa, T., 1443
Yoneyama, H., see Torimoto, T., 3269
Yoo, D.-Y., see Shim, J., 1943
Yoshida, M., see Okada, T., 4419
Yoshida, M., see Taniguchi, I., 2843
Yoshida, N., see Morimoto, T., 4257
Yoshida, Y., Ogata, S., Nakamatsu, S., Shimamune, T., Kikawa, K., Inoue, H. and Iwakura, C.
Decoloration of azo dye using atomic hydrogen permeating through a Pt-modified palladized Pd sheet electrode, 409
Yoshihara, S., Shinozaki, K., Zenbayashi, T., Morino, S., Shirakashi, T., Hashimoto, K., Tryk, D.A. and Fujishima, A.
Nature of the photographic diamond surface phenomenon on boron-doped diamond, 3375
Yoshihisa, Y., see Murata, K., 1501
Yoshimoto, N., see Morita, M., 1335
Yoshimoto, S., see Sawaguchi, T., 2861
Yoshimoto, S., see Taniguchi, I., 2843
Yoshio, M., Nakamura, H. and Xia, Y., 273
Yoshizawa, M., Ito-Akita, K. and Ohno, H.
Evidence of interaction between anion and polyether in the bulk, 1617
Yu, T., see Okada, T., 4419
Yuasa, M., see Okada, T., 4419

Z

Zaban, A., see Aurbach, D., 1135
Zagumennov, V.A., see Nikitin, E.V., 3983
Zak, J. and Kolodziej-Sadlok, M.
AFM imaging of copper stripping/deposition processes in selected electrolytes on boron-doped diamond thin-film electrodes, 2803
Zalewska, A., see Stygar, J., 1437
Zalewska, T., Lisowska-Oleksiak, A., Biallozor, S. and Jasulaitiene, V.
Polypyrrole films polymerised on a nickel substrate, 4031
Zamponi, S., see Giorgetti, M., 4475

Zech, N. and Landolt, D.
The influence of boric acid and sulfate ions on the hydrogen formation in Ni–Fe plating electrolytes, 3461
Zegenhagen, J., see Ziegler, J.C., 4599
Zei, M.S., Wu, K., Eiswirth, M. and Ertl, G.
The effect of different concentrations of chloride on the structure of Cu UPD on Pt(111), 809
Zekovic, L., see Belca, I., 993
Zekovic, L.D., see Belca, I.D., 4059
Žemva, B., see Nakajima, T., 1655
Zen, J.-M., Senthil Kumar, A. and Chang, M.-R.
Electrocatalytic oxidation and trace detection of amitrole using a Nafion/lead–ruthenium oxide pyrochlore chemically modified electrode, 1691
Zenbayashi, T., see Yoshihara, S., 3375
Zeng, X. and Hatton, R.
EQCM study of adsorption of bipyridine on Au polycrystalline electrode using underpotential deposition of Pb as a probe, 3629
Zerbino, J.O.
Ellipsometric and photocurrent characterization of oxide films formed on copper in borax solution with and without benzotriazol, 819
Zhang, J., Zhao, F., Abe, T. and Kaneko, M.
Effect of applied potentials on electron transfer in oxidation and reduction of the $Ru(bpy)_3^{2+/3+}$ couple in Nafion film as studied by potential-step chronoamperospectrometry, 399
Zhang, S., Chang, Z., Xu, K. and Angell, C.A.
Molecular and anionic polymer and oligomer systems with microdecoupled conductivities, 1229
Zhang, W. and Spichiger, U.E.
An impedance study of Mg^{2+}-selective membranes, 2259
Zhang, Z. and Fang, S.
Novel network polymer electrolytes based on polysiloxane with internal plasticizer, 2131
Zhao, F., see Zhang, J., 399
Zheng, T., see Amatucci, G., 255
Zheng, Y., Wright, P.V. and Ungar, G.
Insertion of ionophobic components into amphiphilic low-dimensional polymer electrolytes, 1161
Zhou, A., He, D., Xie, N., Xie, Q., Nie, L. and Yao, S.
Electrochemical quartz crystal microbalance probing the electro-formed and electro-reduced products on a copper electrode in aqueous solutions containing $NaHCO_3$ and Na_2CO_3, 3943
Zhou, J., see Wu, L., 2923
Zhou, X., Ishida, M., Imanishi, A. and Nakato, Y.
Reactions of Si–H to Si–X (X = halogen) bonds at H-terminated Si(111) surfaces in hydrogen halide solutions in the presence of oxidants, 4655
Zhou, X., see Liu, T., 2743
Zhou, X., see Liu, T., 4457
Zhou, X., see Wei, M., 4441
Zhou, Z.-Y., see Wu, Q.-H., 3683
Zhu, L., see Tang, H., 2771
Zhu, L., Tang, H., Harima, Y., Kunugi, Y., Yamashita, K., Kitani, A., Ohshita, J. and Kunai, A.
Electrochemical oxidation of thienylene–silanylene copolymer films in different electrolyte solutions, 2203
Zhu, Y.Y., see Kucernak, A.R., 4483
Ziegler, J.C., Reitzle, A., Bunk, O., Zegenhagen, J. and Kolb, D.M.
Metal deposition on n-Si(111):H electrodes, 4599
Ziegler, J.C., Wielgosz, R.I. and Kolb, D.M.
Pb deposition on n-Si(111) electrodes, 827
Zilberman, G., see Daikhin, L., 3615
Zilberman, G., Tsionsky, V. and Gileadi, E.
Solvent structure at the metal/solution interface and the response of the EQCM, 3473
Zimmermann, C., see Willig, F., 4565
Zón, M.A., see Moressi, M.B., 1669
Zucchini, G.L., see Velichenko, A.B., 4341
Zwilling, V., Aucouturier, M. and Darque-Ceretti, E.
Anodic oxidation of titanium and TA6V alloy in chromic media. An electrochemical approach, 921
Zygadło-Monikowska, E., see Florjańczyk, Z., 1203

PERGAMON

Electrochimica Acta 45 (2000) 29–44

ELECTROCHIMICA Acta

www.elsevier.nl/locate/electacta

Keyword/Subject Index for Volumes 45 (2000)

A

Ab-inito, 131
Ab initio cluster model, 639
Abrasion, 2227
Acetylene hydrogenation, 4309
Acid–base interaction, 1395
Ac impedance spectroscopy, 1901
Activated carbon, 1533
Activation energy, 2019
Active sites, 4127
Active surface states, 4127
Activity coefficients, 969
Adhesion, 2121
Adlayer transition, 731
Adrenaline, 2889
Adsorbates, 575
Adsorbed hydrogen, 3649
Adsorbed ligands, 477
Adsorption, 537, 601, 675, 761, 775, 1623, 2075, 2897, 2961, 3507, 3543, 3629, 3675, 4271, 4279
Adsorption kinetics, 4501
Adsorptive d-band, 4085
Aerogel, 215
AFM, 827, 1491, 4591
Alcohols, 1623
Aldehydes, 2973
Alkali carbonate melts, 1025
Alkaline media, 3943
Alkaline secondary batteries, 1527
Alkaline solutions, 3659
Alkanethiol monolayers, 1885
Alkanethiol|phospholipid bilayers, 1885
Alkanethiols, 4501
Alkene, 3983
Alkylhalides, 1015
Alloy, 1943
Alloy anode, 31
Alloy catalyst, 4211
Alloy deposition, 3691
Alloying effect, 4211
Alloying element, 1933
Al_2O_3, 3413
Alternating copolymers, 1327
Alternating current (ac) impedance spectroscopy, 1491, 2197, 3483, 4151
Aluminium, 1805, 1901
Aluminium alloys, 873
Aluminum, 993, 4059
Aluminum alloys, 881
Aluminum cathode current collector, 2677
Alumite, 4389
Al–Zn–Mg–Fe alloys, 2187
Amalgam formation, 387
Amaranth, 409
Aminopurinethiol, 2869
Amitrole, 1691
Amorphous, 187, 1285
Amorphous alloys, 3389
Amorphous matrix, 1377
Amorphous polymer electrolyte, 1449
Amperometric sensors, 2647, 3951
Amperometry, 2945
Analytical expressions, 3055
Anion effect, 2203
Anion migration, 1617
Anions, 4299
Anisotropic silicon etching, 4635
Anode, 2297, 2461
Anode materials, 295
Anodes, 2279, 4341
Anodic activation, 3295
Anodic deposition, 3423
Anodic films, 993, 1805, 4059
Anodic oxidation, 4629
Anodic partial fluorination, 3005
Anodic Si oxide, 4607, 4615
Anodisation, 921, 3413
Anodisc, 4389
Anodising, 1805
Anomalous codeposition, 3461
Anthraquinone anti-tumor drugs, 3581

PII: S0013-4686(01)00501-1

Anticorrosion, 1921
Aqueous and butanol solutions, 3615
Aqueous borate solution, 931
Aqueous electrolytes, 2467
Aqueous solution, 3337
Aromatic compounds, 4279
Aromatic lithium sulfonylimide salts, 1193
Artificial muscle, 2121
Arylmethylselenides, 3939
Asymmetric viologen, 1127, 4041
Ate complex, 1181
Atomic force microscopy, 2803, 4559, 4629, 4635
Atomic hydrogen, 409
Au(111), 1141
AuCu, 3431
Au electrode, 2897
Au(111) electrode–solution interface, 611
Au(111) single crystal, 2843
Axial texture, 3323
Azo dye, 409

B

2π* backdonation, 639
Bacterial oxidation, 4705
Bandgap, 3345
Barrier, 3213
Battery, 969
B-doped diamond, 3375
B-doped diamond electrodes, 2803
Beam deflection technique, 2781
Bending, 4517
Bending beam method, 4607
Benzene, 4271
Benzoic acid, 1089
Benzotriazol, 819
Benzyl alcohol, 1645
Benzyl thiocyanate, 3005
Bi electrode, 935
Binary solvent mixtures, 1669
Binary systems, 1279
Binuclear, 2061
Biocides, 3639
Biofilm, 1067
Biosensor, 2929, 4373
Bipyridine, 731, 3629
Bismuth, 1623, 3543
Bistability, 3069
Bis(trifluoromethanesulfonyl) amide ion, 1271
Borane, 2991
Boric acid, 3461
Boron doped diamond (BDD), 4691
Boroxine ring, 1175
Branched polysilane, 1007
Breakdown, 3927
Br_2–H_2O mixture, 4663
Brine electrolysis, 4257
Bromide adlayers, 4203
α-Bromo-γ-butyrolactone, 1893
Bubble coverage, 4449
Buffer electrodes, 1963
1-Butanol, 3069
1-Butylpyridinium tetrafluoroborate, 1265

C

Cadmium, 3163
Cadmium telluride, 3355
Ca^{2+} ion, 2939
Calix[4]arenemonoquinone tricarboxylic acid, 2939
Cancer, 2929
Capacitance measurements, 3241
Capacitor, 3813
Capacity, 583
Capillary waves, 685
Carbamate, 3011
Carbon black fillers, 3423
Carbon carriers, 4257
Carbon composite, 2139
Carbon dioxide, 2061, 2995
Carbon nanotubes, 4511
Carbon paste, 4373
Carbon paste electrode, 1105, 2729, 3151
Catalysis, 503
Catalytic hydrogenation, 4299
Cathode, 329, 2461, 3757
Cathode active layer, 4493
Cathode materials, 1781
Cathodic H_2 evolution, 4171
Cathodic oxygen reduction, 1025
Cation coordination, 1255, 1449
Cation radicals, 3939
C_{60}-Dimethyl-(β-cyclodextrin), 4441
C_{60}-[Dimethyl-(β-cyclodextrin)]$_2$, 4441
CdS, 3277
CdS thin films, 623
CdTe, 3225
Cell-impedance, 489
C–F bond, 1655
Chain radical process, 3983
Chalcogenide, 3345
Charge–discharge processes, 1519
Charge propagation dynamics, 3777
Charge-transfer, 2259
Charge transfer processes, 751
Chemical analysis, 87
Chemical doping, 2771

Chemical etching, 4663
Chemically modified electrode, 1639, 1683, 1691, 2623, 4457
Chemical perturbation of the passive–active transition state, 2753
Chemical plating, 4517
Chemisorption, 653, 3105
Chlor-alkali electrolysis, 4251
Chloride, 2187
Chloride baths, 1733
Chloride ions, 3927
Chloride medium, 4525
Chlorine evolution, 2377
Chlorosilanes, 1015
Chronoamperometry, 187, 751, 921, 1095, 3885, 4049, 4697
Chronocoulometry, 775, 3777
Chronopotentiometry, 751, 1105, 3171
cis/trans Isomer ratio, 4291
Clathrate hydrates, 3105
Cleavage, 3537
Cl^- ion incorporation, 1901
Cluster, 4227
CME, 1581
CO adsorption, 3683
Coatings, 1717, 2121
Cobalt, 4419
Cobalt catalyst, 379
Cobalt oxide, 3047
Cobalt spinel, 2719
C_{60}–octasodium calix[8]aryloxy octakis-(propane-3-sulphonate), 2743, 4457
Co-deposition, 3423, 4195
Co(II)/Co(III) complexes, 3675
Co(III) reconstituted myoglobin, 2883
Comb-shaped polyether, 1167
Compact oxide film, 3659
Compatibility, 1187
Complex, 2743
Complex current oscillations, 2753
Complex electrochemical reactions, 3623
Composite material, 4195
Composite polyelectrolytes, 1203
Composite polymer electrolytes, 1481
Composites, 3397, 3877
Composition depth profiles, 1453
Concentrated electrolytes, 3105
Concentrated NaOH, 2823
Concentration of chloride, 809
Condensed phase, 2339
Conductance, 3851
Conducting polymers, 1973, 2273, 2403, 3413, 3423, 3801, 3813, 3833, 3877, 4309
Conducting polypyrrole, 1727
Conductive polymer, 2203
Conductive spectroscopy, 1443
Conductivity, 1049, 1161, 1249, 1271, 1341, 1385, 1467, 1481, 2019, 3127, 3483, 4049, 4329
Confocal Raman spectroscopy, 1405
Conformational rearrangement, 2877
CoNiFe alloy, 3311
σ–π-Conjugation, 2203
Conjugation length, 3841
Constant phase element, 3105
Constituent particles, 881
Contact electric resistance technique, 2029
Controlled potential electrolysis, 3555
Convolution, 3885
Co-polymer, 3851
Copper, 441, 527, 1141, 1361, 2815, 3375, 3675, 3691, 3703, 4127
Copper–cobalt alloys, 1077
Copper complexes, 2803
Copper corrosion, 3639
Copper electrode, 3507, 3943
Copper oxide, 819
Copper selenide, 3737
Corrosion, 3295, 3453, 3993, 4705
Corrosion inhibition, 2677, 2815, 3639
Corrosion protection, 2515
Couette-flow, 1791
Countercation compensation, 3777
Croconic acid, 2697
Cross-linked polymer electrolytes, 1193
Cross-linking, 2911
Cryolite–alumina melt, 2707
Crystal growth, 2559, 3255
Crystalline, 187
Crystallographic structure, 3323
CTAB, 2083
Cu, H_2CO_2, 653
Cu_2O, 3507
$CuPtBr_6$, 1581
Current distribution, 2535
CuZn, 4015
Cu–Zr amorphous catalysts, 3295
Cyanine dyes, 4553
Cyclic reciprocal derivative chronopotentiometry, 457, 761
Cyclicvoltabsorptogram, 2889
Cyclic voltammetry, 295, 387, 751, 845, 913, 1049, 1105, 1113, 1847, 2187, 2289, 2685, 2743, 3063, 3087, 3403, 3555, 3581, 3737, 4271, 4441
Cyclic voltammograms, 1683, 1727
Cycling properties, 197
Cysteine, 4705
Cytochrome *c*, 2869, 2877, 2911
Cytochrome *c* oxidase, 2855

D

Damping, 3703
Decoloration, 409
Decoupling, 1229
Deep-level states, 977
Defectiveness, 4117
Degradation, 1405
Degree of crystallinity, 1399
Density functional calculations, 691
Deposition, 809
Derivative, 2889
Detection, 1067
Determination of DNAs, 477
Devitrification, 3295
Dialkylimidazolium molten salts, 1279
Diamine, 4419
Diamond electrode, 4683
Diaza compounds, 3021
Dicyanomethylene derivatives, 2697
Dielectric dispersion, 1039
Dielectric spectroscopy, 1443
Difference frequency generation, 601
Differential capacitance, 2961, 3489
Differential capacity, 775
Differential pulse voltammetry, 477
Differential scanning calorimetry, 1437
Diffuse double layer, 3483
Diffusion, 527, 1279, 3171
Diffusion coefficient, 1791
Diffusion limitation, 4493
Digestive power, 2933
Digital simulation, 3171
Diglyme, 2019
Dimensionally stable anodes (DSA), 431, 2377
Dimerization reactions, 4409
Dimethylformamide (DMF), 2147
Diphenylbutane, 2991
Direct electron transfer, 2855
Direct methanol fuel cell, 945, 1983, 4319
Discharge capacity, 1773
Disordered carbons, 107, 1607, 1753
Dissolution, 675, 3099
Dissolved oxygen, 2219
3,5-Di-tert-butyl-1,2-benzoquinone, 3029
2,5-di-(-2-Thienyl)-pyrrole, 4049
DMF, 1701
DNA, 2923, 2929
Donor numbers, 2101
Double layer, 2317, 2483
Double layer capacitance, 4501
Dropping mercury electrode, 387
Dry SPE, 1501
DSA, 4351
DSA type electrode, 451
DSC, 1049, 1399, 1467
Dye aggregates, 4559
Dye sensitisation, 4543, 4559
Dye-sensitised, 549
Dynamic response, 1983

E

ECAFM, 2923
ECALE, 3225
EC capacitor, 2685
EC/DMC, 4001
EDAX, 67
Effluent treatment, 2575
EIS, 67
Electrical conduction, 315
Electrical double layer, 3473, 3521
Electric double-layer capacitor, 1533
Electric field effects, 639
Electric neutrality, 3483
Electric vehicles, 2467, 4315
Electrified interfaces, 2339, 3489
Electroabsorbance, 3355
Electroactive species, 3833
Electrocatalysis, 379, 713, 721, 741, 1581, 1639, 1691, 1829, 1911, 2061, 2377, 2743, 4009, 4085, 4127, 4159, 4179, 4187, 4195, 4309, 4315, 4359, 4373, 4457, 4467, 4483
Electrocatalysts, 3283, 4101, 4135, 4227
Electrocatalytic, 4399
Electrocatalytic activity, 1113, 4291
Electrocatalytic effects, 477
Electrocatalytic hydrogenation, 4299
Electrocatalytic mechanism, 1057
Electrocatalytic oxidation, 1057, 2917
Electrochemcial, 1781
Electrochemical behaviour, 1519, 2227, 2697
Electrochemical capacitors, 2483, 4135
Electrochemical carboxylation, 2995
Electrochemical detection, 2933
Electrochemical determination, 1631
Electrochemical discharge, 1655
Electrochemical doping, 2273
Electrochemical electrode, 3573
Electrochemical formation, 3367
Electrochemical impedance spectroscopy, 977, 2515, 2791
Electrochemical implantation, 3367
Electrochemical intercalation, 59, 423, 1753
Electrochemical investigation, 4511

Electrochemical killing, 2917
Electrochemical mass spectrometry, 1645
Electrochemical microfabrication, 2535
Electrochemical micromachining, 2535
Electrochemical modeling, 2595
Electrochemical nanostructuring, 2559
Electrochemical noise, 1763
Electrochemical oxidation, 2203, 3249, 3983
Electrochemical permeability, 2095
Electrochemical processes, 2575
Electrochemical proton insertion, 931
Electrochemical quartz crystal microbalance, 1901, 3615, 3623, 3675, 3683, 3691, 3703, 3725, 3737, 3801, 3841, 3851, 3865, 3877, 3885, 3943
Electrochemical quartz crystal microgravimetry, 3833
Electrochemical quartz crystal nanobalance, 3785
Electrochemical recognition, 2939
Electrochemical reduction, 1015
Electrochemical reductive desorption, 2843
Electrochemical sensor, 1953
Electrochemical stability, 1193
Electrochemical synthesis, 503, 1007, 2121
Electrochemical window, 4691
Electrochemiluminescence, 2437
Electrochemistry, 441, 1741, 1821, 2049, 2443, 2499, 2729, 3163, 4041, 4315
Electrochromic device, 1543
Electrochromic material, 1537
Electrochromism, 2083, 2697, 3403
Electrode, 4373
Electrode double layer, 2961
Electrode impedance, 2961
Electrode kinetics, 457, 4025
Electrode-modification, 2083
Electrodeposited cobalt, 3323
Electrodeposited cobalt alloys, 3323
Electrodeposition, 197, 1733, 2111, 2535, 2559, 2803, 3233, 3255, 3263, 3311, 3345, 3355, 3375, 3389, 3397, 3691, 3711, 3737, 3841, 3959
Electrode position, 4341
Electrodeposition of alloys, 3431, 3461
Electrodeposition of composites, 3431
Electrodeposition of Gd–Co, 2147
Electrodes, 23, 913, 3895
Electroformation products, 3943
Electroless deposition, 3263, 4179
Electroless plating, 3337
Electroluminescence, 4059
Electroluminescence spectrum, 993
Electrolysis of quinones, 3029
Electrolyte decomposition, 3589
Electrolyte flow, 4449
Electrolytes, 23, 1049, 2461
Electrolyte solution, 99, 1135
Electrolyte stability, 2175
Electron avalanche, 4059
Electron hopping, 399, 855
Electronically conducting polymers, 4031
Electronic applications, 2483
Electronic conduction, 2029
Electronic conductivity, 2095
Electronic properties, 2499, 3927
Electronics industry, 2535
Electronic structure, 1875, 4159
Electron probe X-ray micrcroanalysis, 3295
Electron transfer, 2647, 2877, 2953, 3521, 4565
Electron transfer kinetics, 2623, 2903
Electron-transfer mediation, 3581
Electron tunneling, 3497
Electrooxidation, 3939
Electrooxidative polymerization, 3021
Electro-oxydation, 451
Electrophoretic deposition, 3379
Electropolishing, 4615
Electropolymerization, 1581, 1921, 3833, 4049
Electroreduction, 987, 1847
Electroreduction of Gd(III), 2147
Electroreflectance, 3355
Electrosorption, 1121
Electrosynthesis, 3749
Elevated temperature performance, 255
Ellipsometry, 819, 2443, 3659, 4143
Embedded atom method, 699
Energy conversion, 2363
Enhanced effect, 3927
Enzyme, 3573
Enzyme electrode, 2945
Epinephrine, 2889
Epitaxial layer, 3305
Epitaxy, 3233, 3345
EPR and UV-VIS spectroscopy, 3555
EQCM, 899, 1127, 2897, 3473, 3629, 3757
Equivalent circuit, 1999, 3497
Equivalent molar mass, 3943
Etching, 4591
Etching kinetics, 4645
ETH 8045, 2259
ETH 5506, 2259
Ethanethiol, 1141
Ethanol, 3069
Ethylene carbonate, 59, 423, 2019
1-Ethyl-3-methylimidazolium chloride, 3163
1-Ethyl-3-methylimidazolium tetrafluoroborate, 1265
Eumelanin, 1663
Eutectic point, 3157
EXAFS, 4227, 4475
Excitability, 3069

F

Faradaic admittance, 583
Faradaic impedance, 3497
Fast ion conductor, 1249
Father and son coupling, 3087
Fe–25Cr alloy, 899
Fe electrodissolution, 2753
Femtosecond, 4565
Fermi wave-vector, 4085
Ferrite plating, 3337
Ferritic stainless steel, 1933
Ferrocene-modified electrode, 2917
$Fe_{1.99}Ti_{0.01}O_3$, 1999
FeTMPP, 889
Film growth, 899
Films, 2743, 4441
Final cell characteristics, 3
Finite element analysis, 1741
Finite volume method, 3959
Flat band potential, 3255
Flat-band potential, 4655
Flat H–Si(111) surface, 4591
Floating electrode, 379
Flow, 1431
Flow cell, 3355
Flow injection analysis, 2933
Flow-through, 959
Flow-through cell system with a column electrode, 3029
Fluoride, 713
Fluoride salt, 3005
Fluorinated alcohol, 415
Fluorination, 3993
Fluorination treatment, 1773
Fluorine intercalation, 1655
Formic acid, 1057
Fractal dimension, 2111
Fractional factorial design, 4351
Frequency-temperature equivalence, 1039
FTIR, 67, 295, 1727, 2267, 2443
FTIR spectroscopy, 1847, 4271
FT-Raman spectroscopy, 1237
Fuel cells, 1025, 1391, 1741, 4025

G

GaAs(110), 4663
GaAs electrodes, 4577
Gadolinium toluenesulfonate, 2147
Galena, 2729
Galvanic coupling, 881
Galvanised steel, 2165
Galvanoluminescence, 993, 4059
Gas diffusion electrode, 4251, 4257
Gas evolution, 959
Gas-evolving electrodes, 4449
Gd–Co alloy film, 2147
Gel electrolytes, 1307, 1327, 1341, 1347, 1371, 1537
Gelled SPE, 1501
Gel polymer, 4001
Gel-type polymer electrolytes, 2101
Glass transition, 1229, 1243, 1473
Glass transition temperature, 1285, 1617
Glutathione, 3555
Gold, 601, 3283, 3305, 4127
Gold–cobalt electrode, 1113
Gold electrodes, 1847, 2075, 4203
Gouy–Chapman, 685
Gradient catalyst, 4493
Graphite, 23, 99, 423, 1655, 1893, 3151
Graphite electrode, 2929
Graphite–epoxy composite, 789
Graphite intercalation compound, 59
Graphite–lithium, 87
Graphite + polymer composite electrodes, 797
Growth, 1973

H

H-adatom, 4085
Halide ion action, 2753
Halides, 3675
Halogenated acid, 4457
Hanging mercury drop electrode, 1095
[2H] benziso-1,2-thiazol-3-one, 4525
[2H] benziso-1,2-thiazol-3-one S-oxide, 4525
H chemisorption, 4075
Heme rotation, 2903
Heterogeneous catalysis, 653
Heterogeneous electron transfer, 3497
Heterogeneous kinetics, 1669
Hexachloroplatinic acid, 3711
High B_S film, 3311
High-energy-density batteries, 1519
High ρ film, 3311
Highly oriented pyrolytic graphite, 865
High rate capability, 3099
High-voltage cathode materials, 295
Hillocks, 4635
Hofmann rearrangement, 3011
Hollandite, 2211
HOPG, 2923, 4483

Hybrid, 3081
Hydration, 2267, 3063
Hydration of halide ions, 659
Hydrocoupling, 2991
Hydrofluoric acid, 2219
Hydrogen, 1943, 3927
Hydrogen adsorption/desorption, 3205
Hydrogen and oxygen evolutions, 431
Hydrogen and oxygen isotherms, 4143
Hydrogenation/dehydrogenation, 483
Hydrogen-bond, 1223
Hydrogen bonded complex, 2869
Hydrogen bonding interaction, 1395
Hydrogen concentration profile, 2781
Hydrogen evolution, 3205, 4009, 4159, 4195, 4299
Hydrogen evolution reaction, 3375, 4151, 4483
Hydrogen formation, 3461
Hydrogenolysis, 409
Hydrogen oxidation, 4299
Hydrogen peroxide, 889, 1639
Hydrogen storage, 4511
Hydrogen storage alloy, 1773, 3973
Hydrosilylation, 2131
Hydrous oxide film, 3659
Hydroxide ions, 3507
Hydroxide solutions, 3105
Hypo-hyper-*d*-interionic catalyst, 4085
Hysteresis, 3865

I

ICP-MS, 161
Illumination, 4015
Image formation, 1549
Imidazolium salt, 1291, 1295
Imide anion, 1271
Immiscible electrolyte solutions, 583
Impedance analysis, 2259
Impedance measurements, 1781
Impedances, 935, 1773, 1837, 1999, 3277, 4015
Impedance spectroscopy, 845, 1039, 1211, 1437, 2029, 3497, 4031, 4171, 4501
Improved PEM fuel cell, 4329
IMPS, 3277
Indirect electrochemical synthesis, 4525
Indium deposition, 4673
Indium oxide, 1595
Indium phosphide, 4673
Induction heating, 451
Industrial processes, 2377
Infrared, 2267
Infrared spectroscopy, 1255, 1437, 1701, 3205
Ink type electrode, 889
Inorganic fillers, 1203, 1473
Inorganic–organic matrices, 1377
Inorganic–organic polymers, 1211
Insertion electrodes, 351
In-situ absorption spectra, 1727
In situ conductance, 1811
In situ FTIRS, 2897
In-situ spectroscopy, 1717
In situ STM, 2861
In-situ techniques, 2443
In situ time-resolved UV-vis subtractive reflectance spectroscopy, 2877
In situ XRD, 67
Integral equations, 2317
Intensity modulated, 549
Intensity-modulated photocurrent spectroscopy, 4543
Intercalation, 131, 243, 273, 329, 1893, 2595, 3171
Intercalation cathode, 285
Intercalation electrodes, 1781
Interdigitated flow-fields, 4319
Interface, 23, 1999
Interface passivation, 3563
Interface stress, 575
Interfacial coupling, 3649
Interfacial films, 225
Interfacial properties, 1481
Interfacial resistance, 1301, 1307, 2197
Interfacial structure, 2219
Interfacial tension, 685
Interfacial viscosity, 3649
Interference, 623
Internal plasticizing chains, 2131
Internal porosity, 1607
Inverse spinel, 295
In vivo electrochemistry, 2623
Ion-association, 1313
Ion conductivity, 1223
Ion–dipole interaction, 1617
Ion exchange, 3801
Ionic associations, 1327, 1437
Ionic conductivity, 1167, 1175, 1181, 1203, 1265, 1279, 1285, 1291, 1295, 1321, 1327, 1335, 1361, 1371, 1417, 1431, 1463, 1473, 1527, 1537, 1617, 2131, 3081, 3563
Ionic defects, 2029
Ionic desorbtion, 3489
Ionic exchange, 1953
Ionic liquid, 1295
Ionic partition diagram, 2647
Ionic transport, 1805
Ionode, 2647
Ionomer, 1301
Ions, 1623, 3543

Ion transport, 2083
IRAS, 1089, 2075
Iridium dioxide, 451, 4351, 4467
Iridium oxide, 431
Iron corrosion, 1717
Iron nitride film, 3367
Irreversible capacity, 1607
IR spectroscopy, 1121
Isopropanol, 451
Isoquinoline, 987
ITIES, 2647
ITO electrode, 797

J

Japan, 4315
Jellium, 2317

K

Kelvinprobe, 2515
β-Keto carboxylic acid, 2995
Ketones, 2049
Kinetic model, 2791
Kinetics, 1753, 2049, 2219, 2289, 3087
Kinked step surfaces, 4263
KOH, 4645
KS-6, 1533

L

$LaNiO_3$/Ni–PVC composite, 741
Lanthanide doped polymer, 1463
Lanthanide doped sol-gel, 1467
Lanthanum gallate, 2095
Lateral morphology, 1453
Lattice energy, 1291
Lattice fluid model, 3157
Lattice-gas modeling, 645
Laves phase alloy, 3099
Layered oxides, 243
Layered rocksalt, 329
Layered semiconductor, 4559
Leaching, 2729
Lead chloride, 2729
Lead dioxide, 713, 4341
Lead ferrites, 1105
Lead–ruthenium oxide pyrochlore, 1691
Leuco-methylene blue film, 3785
Lewis acid, 1181
$LiBF_4$, 1701
$LiCF_3SO_3$, 1237, 1243
$LiCo_{0.5}Al_{0.5}O_2$, 187
$LiCoO_2$, 187
$LiCoVO_4$, 295
Li diffusion, 187
Life, 3099
Ligand dissociation, 2903
Li-ion cell, 255
Li^+ ion conductor, 1181
LiI–(PEO), 1431
Li metal and Li ion batteries, 67
$LiMn_2O_4$, 2197
$LiMn_2O_4$/C Li-ion system, 255
Linear sweep voltammetry, 1733, 3063
$LiNiVO_4$, 295
^7Li NMR, 243
Lipase activity, 2933
Lipid bilayer membrane, 2855
Li polymer batteries, 2101
Lipophilic anionic sites, 2259
Lipophilicity, 2647
Liquid, 4577
Liquid crystal, 1161
Liquid retention, 1307
Lithiated graphite, 67
Lithiated transition metal oxides, 161
Lithium, 59, 273, 865, 873, 1223, 1893, 2019
Lithium alloys, 31
Lithium and proton NMR, 1237
Lithium batteries, 51, 107, 131, 215, 243, 273, 285, 315, 1135, 1175, 1193, 1321, 1341, 1417, 1501, 1509, 2139, 2197, 2211, 3171, 3589, 3757
Lithium cobalt dioxide, 489
Lithium cobalt manganate, 315
Lithium conductor, 2139
Lithium electrodes, 67
Lithium imide solutes, 2677
Lithium incorporation, 873
Lithium insertion, 3, 121, 351, 3141
Lithium intercalation, 197
Lithium ion, 235, 969, 1161, 1513
Lithium-ion batteries, 3, 31, 99, 121, 151, 161, 329, 1509, 1607, 1753, 1781, 2175, 2461, 3127, 4001
Lithium manganese dioxide, 3141
Lithium manganese oxide, 285
Lithium manganese spinel, 2175
Lithium nickelate, 243
Lithium passivation layer, 1491
Lithium perfluorinated polyimide, 1187

Lithium polyelectrolytes, 3563
Lithium polymer battery, 1509
Lithium rechargeable batteries, 2677
Lithium secondary batteries, 295
Lithium storage alloys, 31
Lithium triflate, 1249
Li^+ transference numbers, 1175, 2101
Localised corrosion, 2165, 2753
Local structure, 107
Low frequency resistance, 977
Low molecular-weight organic gel, 1537
Luminescence, 1555
Luminescent ions, 561

M

Macrocycles, 2061
Magnesium alloy electrode, 3973
Magnesium hydroxide deposit, 1837
Magnesium insertion, 351
Magnesium metal, 351
Magnetic properties, 3323, 4389
Manganese dioxide, 215, 2211
Manganese–molybdenum oxide, 2297
Manganese oxide, 215
Manganese oxide electrode, 225
Manganese oxides, 273, 2175
Mars, 1513
Mass sensitivity distribution, 3725
Mass-spectrometry, 3029
Mass transfer, 945
Mass transport, 1067, 1837, 3777
Mathematical model, 959, 1077
Matrix materials, 3397
MCFC, 1025
MCMB, 121
Mean-field approximation, 645
Mechanism, 4591
Mechanism Mo–Ni alloys, 4151
Mechano-electric oscillations, 583
Mediators, 1821, 2917
melting, 1473
Melting point depression, 3157
Membrane, 1741
Membrane oxygen electrode, 469
ω-Mercaptoalkanoic acids, 537
2-Mercaptobenzoxazole, 2815
2-Mercaptopyridine, 2861
4-Mercaptopyridine, 2861
Mercury surface, 537
Mesocarbon micro-beads, 121
Metal/aqueous solution interface, 3521
Metal chalcogenides, 3749
Metal dissolution, 899
Metal dot arrays, 3263
Metal electrodes, 1885, 2387
Metal ions, 477
Metal–liquid interface, 3453
Metal porphyrin polymer, 3021
Metal sulfides, 4705
Methacrylate copolymer, 1443, 1543
Methanol, 451, 3543
Methanol cross-over, 4319
Methanol oxidation, 653
Methanol permeation, 4237
Methanol tolerance, 4237
Methyl chloroformate, 1893
2-Methyl-1,4-naphthoquinone, 3029
3-Methylthiophene, 3851
Methylviologen, 797
Mg^{2+}-selective membrane, 2259
Michaelis–Menten kinetics, 1691
Microbially induced corrosion (MIC), 3639
Microcrystals, 2227
Microdecoupled conductivity, 1229
Microelectrochemistry, 483
Microelectrode, 1683
Microelectrodes, 3483
Microelectrode sensors, 2437
Microemulsions, 503
Microfabrication, 2437
Microgravimetry, 3777
Micropatterning, 3725
Microstructure of composites, 3431
Mineral sulfide oxidation, 2729
Mixed catalyst, 4419
Mixed conductors, 2095
Mixed oxides, 4431
Mixed potential, 2781
Mixed solvents, 2019
Mixed valence vanadium oxide, 197
Mixed-valent molybdenum oxide, 1683
MMC, 3431
$MnNi_{3.55}Co_{0.75}Mn_{0.4}Al_{0.3}$ alloy, 483
Mn, 255
MnO_x/C composites, 913
Models, 969, 1821, 2403, 3055
Model system, 881
Modified electrodes, 1829, 3379, 3801, 3951, 4179, 4341
Modified membranes, 4329
Modified surface, 4143
Molal conductivity, 1437
Molecular assembly system, 2953
Molecular charge transfer, 2339
Molecular dynamics, 1425
Molecular dynamics simulations, 2317

Molecular organisation, 1161
Molecular semiconductor, 4697
Molten salts, 441, 469, 1249, 1271, 1291, 3163
Molybdenum trisulfide, 3877
12-Molybdophosphoric acid, 1639
Monodisperse nanoparticle, 3269
Monolayer, 1829
Monomer–dimer, 4041
Monosaccharides, 2973
Monosilyl, 2771
Monte Carlo simulations, 645, 659, 699, 2317
Morphological factors, 3249
Mössbauer, 243
Mössbauer spectroscopy, 51
Multi-ion, 3959
Multilayer, 1829
Multiple sulfonate anion, 3813
Multi-sensing devices, 2437
Multivalent cations, 1335
m-Xylene, hydrogenation, 4291
Myoglobin, 2883, 2903

N

N-Acylurea, 3011
NAD^+, 3151
NADH, 3151
NADH electrocatalytic oxidation, 3951
NAD^+-modified electrode, 3151
Nafion 117, 1741
Nafion®, 415, 797, 2267, 3765, 4219, 4329
Nafion film, 399
n-Alkanethiols, 1127
Nanocomposite, 1481
Nanocrystalline, 549, 1595, 4543
Nanocrystalline solar cells, 4553
Nanoparticles, 431, 3277, 4483
Nanostructure, 4117
Nanostructuring, 2387
Nanowire, 4389
Naphthalene sulfonate, 3813
Natural convection, 3959
n-Butanol adsorption, 3473
n-Doping, 2273
Neodymium (III), 1555
Network analysis, 3703
Network polymer, 3081
Network polymer electrolytes, 2131
Neuroscience, 2437
Neutralization, 1291
Neutron diffraction, 285, 1449
Neutron scattering, 107
Nickel, 4031
Nickel anode, 3993
Nickel–chromium alloys, 2791
Nickel/cobalt cyclam complexes, 855
Nickel–cobalt hydroxides, 4187
Nickel electrodes, 2111
Nickel hexacyanoferrate, 2083, 3777
Nickel(II), 2061
Nickel–phosphorus, 4179
Nickel–polyester electrode, 4187
Nickel substrate electrode, 4031
Ni–Co alloys, 1733
Ni–MH battery, 483
Ni–MH battery, 3973
Niobium pentoxide, 4351
Nitrosobenzene anion radical, 3555
Noise spectrum, 1763
Nonaqueous magnesium electrolytes, 351
Non conventional electrolytes, 2611
Non-faradaic process, 1811
Non-permselectivity, 3801
n-Si(111) electrodes, 827
Nuclear magnetic resonance, 3029
Nucleation, 865, 873, 1973, 2559, 3163, 3255
Numerical analysis, 489

O

Octadecanethiol, 4041
Ohmic drop, 789, 4493
Oligo(ethyleneoxide), 1543
Oligomers, 3841
Oligomer systems, 1229
Oligothienyls, 2771
Oligothiophene, 1543
On-line mass spectrometry, 4279
On-site power stations, 4315
Open-circuit potential transient, 2781
Operating conditions, 1983
Optoelectrochemical method, 4143
Order/disorder, 131
Order–disorder–order, 731
Organic coatings, 2515
Organic compound adsorption, 935
Organic conductor, 4697
Organic electrolytes, 2019, 3127, 3589
Organic electrolyte solution, 2197
Organic gels, 3563
Organic/inorganic hybrids, 1555
Organic pollutants, 2575
Organoaluminum compounds, 1203
Organocobalt, 4475
Organophosphorus compounds, 3983
Organosulfur compounds, 4525

Orientation, 935
ORMOCERs, 1377
Oscillations, 3069, 4517
Overoxidation, 1727
Overpotential deposition, 4075
Overvoltage at BDD electrodes, 4691
Oxalic acid, 993
Oxidation, 1039, 2889, 2923, 3205, 3283, 4271, 4399, 4431, 4517
Oxidation potential, 1663
Oxide electrodes, 2377
Oxide film, 2791
Oxide–hydride formation, 4159
Oxide mixtures, 2719
Oxides, 23
Oxide solubilities, 469
Oxidizable metals, 1921
Oxidized layer, 3993
Oxidizing agent, 4645
Oxobasicity index, 469
Oxyethylene units, 1167
Oxygen, 987, 1943, 3345, 3581
Oxygen cathode, 4251
Oxygen diffusivity, 2823
Oxygen evolution, 713, 741, 1911, 2279, 2297, 4359
Oxygen evolution reaction, 4187, 4467
Oxygen reduction, 379, 415, 721, 889, 2289, 3305, 4025, 4203, 4211, 4219, 4227, 4419
Oxygen reduction catalyst, 4237
Oxygen reduction cathode, 4257
Oxygen reduction reaction, 4493
Oxygen solubility, 2823
Ozone, 713

P

PAH, 845
Palladium, 1645, 3305
Palladium electrodeposits, 4117
PAN, 1361
Particle pulverization, 3099
Particle size effect, 4211
Passivating layer, 1893
Passivation, 87, 1717, 4645
Passive films, 1875, 2029, 2499, 4015
Passive layer, 1301
Passivity, 1571, 3927
Pb, 3629
Pb deposition, 827
$PbO_2 + CoO_y$ composites, 2279
Pd foil electrode, 2781
Pechini, 4467
Pechini method, 4351
PEDOT films, 1921
Peltier heating, 2707
PEM fuel cells, 889, 2467
PEO, 1473
Percolation, 789
Permeability, 845
Permittivity, 2259
Permselectivity, 3801
Perovskite anodes, 741
Peroxide ion, 59, 4431
Perylene, 4565
PFG-NMR, 1341
PGSE NMR, 1313
pH, 2855
Phase-boundary movement, 489, 865
Phase changes, 1519
Phase diagrams, 131
Phase equilibrium, 1631
Phase separation, 1347
Phase tranformation, 2227
Phase transition, 675, 3785
Phenols, 4373
Phenothiazine derivatives, 3951
Phenylacetylene, 2991
Phosphate inhibitors, 1717
Phosphoric acid, 1385, 1391, 2945, 4219
Photocatalysis, 2363
Photocurrent, 819, 3277, 3355
Photocurrent spectroscopy, 2219
Photo-decomposition, 1571, 4015
Photo-dissolution, 1571
Photoelectrochemistry, 549, 1595, 2363, 3213, 3375, 3403, 4697
Photoelectrode, 3269
Photoelectron spectroscopy, 4615
Photoinduced electron transfer, 1549
Photoluminescence, 3345, 4629
Photon correlation spectroscopy, 1409
Photorewritable image, 1549
Photovoltaic, 549
Phthalocyanine, 4697
Physical diffusion, 399
Piezoelectric sensors, 3785
Pitch fibres, 423
Pitting, 2187, 4015
Pitting corrosion, 881
Plasticizer, 1701
Platinum, 1645, 1943, 2929, 3659, 4127, 4219
Platinum catalyst-electrode, 4299
Platinum electrode catalyst, 4257
Platinum electrodes, 1057, 3649, 4203, 4271, 4279
Platinum films, 3711
Platinum oxide, 3659
Platinum oxides, 3063
Platinum phthalocyanine, 2227

PNBA, 2897
Poly(acrylonitrile), 1237, 1243, 1249, 1361, 1371
Poly(acrylonitrile-co-lithium methacrylate) (P(AN-co-LiMA)), 1301
Polyalkylsilyne, 1007
Polyaniline, 3865, 3877, 4171
Polyaniline pattern, 1549
Polyanion conductors, 1229
Poly(benzimidazole), 1395, 4219
Poly(3-dodecylthiophene), 3841
Polyelectrolyte film, 845
Poly(epichlorohydrin), 1527
Polyethylene glycol, 1211
Poly(ethylene oxide), 1203, 1223, 1285, 1371, 1527, 1617, 2911, 3081
Polyethylenimine, 1385
Polyfurane, 1973
Poly(MAN-alt-$(EG)_4$DVE), 1327
Polymer alloy, 1187
Polymer-coated electrode, 4009
Polymer composite electrolyte, 1473
Polymer electrode, 4309
Polymer electrolyte fuel cell, 1943
Polymer electrolyte interface, 1491
Polymer electrolytes, 1161, 1175, 1187, 1211, 1249, 1255, 1265, 1301, 1313, 1347, 1361, 1371, 1385, 1417, 1533, 2139
Polymer–gel electrolyte, 1543
Polymer gels, 1347, 1409
Polymeric electrolyte, 1335, 1791
Polymer–inorganic interface, 1425
Polymer-in-salt electrolytes, 1237, 1243
Polymer network, 1307
Polymer proton conductor, 1399
Polymers, 23, 1229
Polymer solid electrolyte, 1167
Polymethacrylonitrile, 1255
Poly(methylalkoxysiloxane), 1049
Poly(3-methylthiophene), 1811
Polymorphic phases, 3785
Poly(*o*-toluidine), 3885
Polyoxometalate, 1829
poly(pentafluorophenyl 3-(pyrrol-1-yl)propionate), 3823
Poly(pyrrole), 855, 1953, 2121, 3413, 3801, 3813, 4031, 4179
poly(pyrrole-*N*-propionic acid), 3823
Poly(silamine), 1391
Poly(styrene sulfonic acid), 1405
Polythiophene S,S dioxide, 2273
Poly(vinylferrocene), 3895
Poly(vinylidene fluoride), 1347, 1405
Pore size distribution, 2241
Porous electrode impedance, 2241
Porous electrodes, 959, 2111
Porous film, 921
Porous layer, 1837
Porous silicon, 561
Porous SPE, 1501
Porphyrin, 3021
Positron annihilation lifetime spectroscopy, 1243
Potential of zero total charge (pztc), 629
Potential step, 4025
Potential-step chronoamperospectrometry (PSCAS), 399
Potentiodynamic behaviour, 2973
Potentiostatic current transient, 489
Pre-polarization, 2923
Pressure effect, 3157
Pretreatment, 3263
Primary lithium battery, 1655
Prismatic, 235
Probe beam deflection (PBD), 1953, 3885
Programmed current, 761
Programmed currents, 457
2-Propanol, 1623, 3543
Propidium iodide, 2917
Propylene carbonate, 1893
Proteins, 1821
Protein voltammetry, 2623
Proton conducting membrane, 1405
Proton conduction, 1391, 1395, 1409
Proton conductor, 1377, 1385
Proton-exchange membrane fuel cell (PEMFC), 415
Proton reduction, 4009
Proton transfer, 2267
Prussian-blue, 789
Prussian-blue films, 751, 3765
Pseudocapacitance, 2685
PSS, 845
Pt(111), 809
Pt alloys, 4101
Pt electrode, 3683
Pt(111) electrodes, 629
Pt particles, 3283, 4171
Pt–Ru catalyst, 4319
Pt single crystal surfaces, 4263
p-Type conductivity, 2095
Pulsed laser deposition, 187
Pulse-plating, 1077
PVC/PMMA, 4001
PVDF, 1701
P(VdF/HFP), 1341
Pyramids, 4635
Pyrazine, 2075
Pyridine, 611
Pyridine adsorption, 3473
Pyridine adsorption on gold, 3615
Pyridinethiol, 2843

Pyrolysis, 379, 4419
Pyrolysis technique, 3047
Pyrophosphate, 3691
Pyruvic acid, 2945

Q

Quantum calculations, 659
Quantum chemistry, 3521
Quartz crystal microbalance, 2815, 2869, 3639, 3649, 3659, 3757, 3765, 3813, 3823
Quartz crystal microgravimetry, 3749
Quartz crystals, 899
Quartz resonant frequency, 3895
Quinoline, 987
Quinone, 2933

R

Radical-anions, 2697
Radical-cation, 3983
Radical cation stabilities, 4409
Raman spectroscopy, 1121
RDE method, 4025
Reaction, 2131
Reaction center, 1821
Reactivity, 1015, 3939
Rechargeable batteries, 2467
Rechargeable magnesium batteries, 351
Redox catalysis, 1015
Redox couples, 1095
Redox mediator, 2883
Redox potential, 2883, 2903
Redox probes, 1885
Redox processes, 243
Redox reaction, 1067, 2911
Redox sites, 855
Redox species, 1683
Redox switching, 3801
Redox transformation, 1811
Redox transitions, 3403
Reduction, 503
Reduction mechanism, 4475
Reduction of CO_2, 4263
Reduction potential, 1663
Reflectance spectroscopy, 3403
Regioregular oligothiophenes, 4409
Regioselectivity, 3005
Relaxation, 3865
Repassivation kinetics, 1933
Repulsive interactions, 575
Resonance frequency, 899
Reversible couple, 1089
Review, 351
Roll-off frequency, 1763
Roll-off slope, 1763
Room temperature, 441
Room temperature molten salt, 1265, 1295
Rotating-disc, 1791
Rotating-disk electrodes, 721, 3573, 4457
Rotating ring-disk electrode, 415, 2175, 2289
R.R.D.E., 2823
$Ru(bpy)_3^{2+/3+}$, 399
Ru complex, 1549
$(Ru + Ir)O_x \cdot nH_2O$, 2685
Ruthenium, 2289, 3021
Ruthenium chalcogenide, 4227
Ruthenium oxide, 2719, 4135, 4195
Ruthenium-red, 4009

S

Salt-doped polymer electrolyte, 1453
Salts–polymer interactions, 2101
Sb adatom, 3683
Scanning electrochemical microscopy (SECM), 3725, 4483
Scanning Maxwell stress microscopy, 2953
Scanning tunneling microscopy, 99, 527, 2387, 2815, 3213
Scanning vibrating electrode technique (SVET), 2165
Scavenging, 3555
SCF-MO, 3055
Schottky barrier, 4673
Scratching electrode technique, 1933
SDS micelles, 1921
Sea-water, 1837
Seawater electrolysis, 2297
Secondary battery, 2019
Secondary lithium batteries, 2595
Second harmonic waves, 623
Second order surface reactions, 3087
Seebeck coefficient, 2707
SEI, 87
Selective adsorption, 2843
Selective response, 2939
Self-assembled monolayers, 1141, 1491, 2861, 3497, 4501
Self-assembly, 845
Self-diffusion, 1313
Self diffusion coefficient, 1321
Self-diffusivity, 1327
Self-discharge, 2781, 3973

Semiconducting, 1571
Semiconducting films, 977
Semiconductor corrosion, 4673
Semiconductor electrochemistry, 3205, 4705
Semiconductor electrodes, 561
Semiconductor film deposition processes, 3749
Semiconductor nanoparticle, 3269
Semiconductors, 819, 1999, 3255, 3345, 4577, 4655
Sensor, 4683
SER spectroscopy, 1847, 2897, 3295
Sidechain dipoles, 1229
Silicon, 2219, 3249, 4645
Silicon oxide layer, 3263
Silicotungstic acid, 4329
Siloxyaluminate polymer, 1181
Silver, 527, 3703
Silver electrodes, 3225, 4203
Silver single crystal, 675
Simulations, 131, 1425, 2049
Single crystals, 601, 1623, 2075, 3117, 3225, 3233, 3305, 3543
Single-ion conducting polymer, 1443
Single-ion conduction, 1187
Single spherical particle, 483
Si oxide etchback, 4607
Si⟨111⟩ surfaces, 3241
Size quantization effect, 3269
Smooth nickel, 4143
SNIFTIRS, 611, 4041
Sodium, 423
Sodium-β-alumina, 1631
Sodium borohydride, 2991
Sodium countercation, 3765
Soft magnetic film, 3311
Solar cells, 2647, 3355, 4543
Solar energy storage, 2467
Sol–gel, 215, 1911, 4359, 4467
Sol–gel films, 1595
Sol–gel method, 4351
Sol–gel process, 4135
Sol–gel technique, 1639
Solid polymer electrolytes, 945, 11501, 509, 1527, 4517
Solid solution mechanism, 315
Solid-state cells, 1963
Solid state lithium polymer battery, 1509
Solid state potentiometry, 1631
Solid-state redox reactions, 151
Solvation, 1313, 3851
Solvent effects, 1669, 3011
Solvents at interface, 3473
Sorption isotherm, 4117
Sorption of anions, 3777
Spacecraft batteries, 1513
Spatial heterogeneity, 1443
Specific cations, 3537
Spectro-electrochemical cell, 591
Spectroelectrochemical techniques, 2889
Spectroelectrochemistry, 1121, 2697, 2883, 4475
Spectroscopy, 3213
Spinel electrode, 931
Spinel oxides, 1911
Spinels, 315, 3337, 4431
Spinel type electrodes, 4359
SPM, 4655
Squaraine dye, 4559
SQUID magnetometer, 3453
Stability, 2911
Stage transformation, 865
Standing waves, 3725
Step bunches, 4635
Step fluctuations, 527
Stepped surfaces, 629, 4263
Stereoselectivity, 4291
Stoichiometry, 1105
Strain rate, 3537
Stress corrosion cracking, 3537
Stress corrosion susceptibility, 1933
Stretching, 1431
Strong acid, 1395
Structural characterization, 3241
Structure-conductivity relationships, 1417
Study, 3623
Substrate supported nanosystems, 2559
Subtractively normalized interfacial infrared spectroscopy, 3589
Sulfide, 2843
Sulfonamide, 3081
Sulfonamide salt, 1285
Sulfonic surfactant, 3413
Sulfon/sufonamide functions, 1377
Sulfur addition, 721
Sulfur diffusion, 3355
Sulphate ion, 1901
Sulphur adsorption, 1847
Sulphur dioxide, 1847
Sulphur modified gold electrode, 3785
Supercapacitor, 2483
Supercritical fluids, 2611
Superhydrophilicity, 4683
Superoxide, 2049
Superoxide ion, 987
Supporting electrolyte, 3483
Suppression of pyramids, 4645
Surface analysis, 1733
Surface area, 4135
Surface characterization, 2719
Surface charge, 575
Surface chemistry, 67
Surface enhanced Raman spectroscopy (SERS), 3507

Surface film, 99
Surface landers, 1513
Surface mobility, 3537
Surface modification, 1773
Surface modified electrodes, 797
Surface morphology, 2111
Surface pH, 3461
Surface stress, 575
Surface structure, 2387
Surface-termination bond, 4655
Surface treatment, 3993
Surface X-ray diffraction, 4203
Surfactants, 503
Swelling, 1307
Synchrotron, 591
Synthesis, 1973
Synthetic polymer, 1663

T

Tafel plots, 2289
Tailor-made surface, 4101
Temperature, 2855
Temperature and concentration effect, 2823
Template electrodeposition of cobalt, 4389
Template reverse pulse electrodeposition of gold, 3117
Termination of BDD surface, 4691
Tertiary current distribution, 3959
Tetrafluoroborate, 441, 3163
Tetragonal lithium manganite, 3141
TG, 1399
TGA, 1467
Thallic oxide, 3233
Theoretical study, 653
Thermal behavior, 197
Thermal decomposition, 3063
Thermal modeling, 2595
Thermal oxidation, 3993
Thermal property, 1321
Thermal stability, 1463, 2019
Thermo-currents, 3453
Thermodynamic measurements, 1963
Thermodynamics, 969, 1753, 2403
Thermodynamics and stability ranges of low-dimensional phases, 2559
Thermodynamic stability, 1631
Thermogalvanic cell, 2611
Thickness, 235, 1067
Thienylene–silanylene copolymer, 2203
Thin films, 187, 1453, 1533, 1911, 3337, 3737, 4359, 4431
Thin film stress, 4607
Thin polymer films, 4171
Thiol monolayers, 537
Thiophene, 4329
Thiophene derivative, 2273
Thiophenol, 2861
Thiouracil, 2869
Tin, 31
Tin borophosphate glass, 51
Tin oxide, 51, 977
TiO_2 photocatalysis, 4683
Tiron, 1953
Titanium, 1211, 2121, 3047, 4691
Titanium alloy, 921
Titanium dioxide, 4543, 4553, 4565
TLM-PSD, 2241
TMPD, 1669
Trace metal analysis, 4683
Trace metals, 2437
Transformation, 4399
Transient behaviour, 1983
Transition metal sulfides, 4237
Transpassive dissolution, 2791
Transport in polymer films, 3833
Transport mechanisms, 1279
Transport number, 1193
Trichloroalkylsilane, 1007
Tungsten, 1875
Tungsten alloys, 3389
Two-dimensional condensation, 2961
Two-dimensional cross-linking, 3269
Type 304 stainless steel, 3927
Tyrosinase, 4373

U

Ultracapacitor, 2483
Ultramicrogravimetry, 4049
Ultrasonic field, 3117
Underpotential deposition, 691, 699, 1141, 4075
α,β-Unsaturated carboxylic acid, 2995
Unsteady diffusion, 1791
Unsupported catalysts, 4319
Upd, 809, 3225, 3629
UPD tin, 1057
Urea, 2945
Uridine, 675

V

Vanadium oxide, 215
Vanadium pentoxide, 187, 215, 3757
Vibrational spectroscopy, 601, 1409
Vinyl triflate, 2995
Viscosity, 2019
Volcano plots, 4075, 4085
Volmer–Weber growth, 827
Voltage, 2483

Voltametry, 921
Voltammetric characterization, 741
Voltammetry, 1089, 1127, 1885, 3777
Voltammogram, 4263
VTF equation, 2131

W

Wall-jet electrode, 3675
Water, 3543
Water contamination, 1135
Water electrolysis, 4187
Water management, 1741
Water-soluble calixarene, 2939
Watersplitting photoelectrode, 4673
Water uptake, 4329
Wave packet motion, 4565
Welding effect, 2187
Wide-angle X-ray diffraction, 1167
Wired enzymes, 2623
Work function, 691
WSe_2, 3213

X

XANES, 4475
Xerogel, 215
XPS, 67, 721
X-ray, 1399
X-ray diffraction, 591
XRD, 151, 295

Z

Zeolite, 3379
Zinc, 3691
Zinc oxide, 3345
Zirconium alloys, 1039
ZnO, 1571
Zr–Ni amorphous alloys, 4159

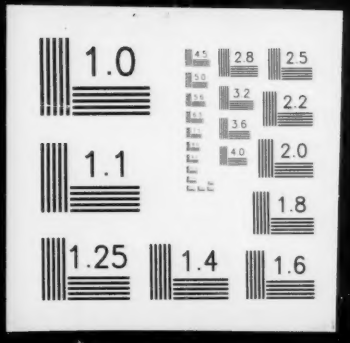
1.0
1.1
1.25
1.4
1.6
2.8
2.5
3.2
2.2
3.6
2.0
4.0
1.8